



CFD STUDY FOR A TWIN-ENGINE AFTERBODY MODEL INTERCEPTOR  
FIGHTER

A THESIS SUBMITTED TO  
THE SCHOOL OF GRADUATE STUDIES  
OF  
UNIVERSITY OF TURKISH AERONAUTICAL ASSOCIATION

BY

DAVID MUHIRE

IN PARTIAL FULFILLMENT OF THE REQUIREMENTS  
FOR  
THE DEGREE OF MASTER OF SCIENCE  
IN  
AEROSPACE ENGINEERING

AUGUST 2024



CFD STUDY FOR A TWIN-ENGINE AFTERBODY MODEL INTERCEPTOR  
FIGHTER

A THESIS SUBMITTED TO  
THE SCHOOL OF GRADUATE STUDIES  
OF  
UNIVERSITY OF TURKISH AERONAUTICAL ASSOCIATION

BY

DAVID MUHIRE

IN PARTIAL FULFILLMENT OF THE REQUIREMENTS  
FOR  
THE DEGREE OF MASTER OF SCIENCE  
IN  
AEROSPACE ENGINEERING

SUPERVISOR: Assoc. Prof. Dr. Ali Ruhşen ÇETE

12 AUGUST 2024

**Approval of the thesis:**

**CONCEPTUAL DESIGN OF A TWIN ENGINE AFTERBODY MODEL  
INTERCEPTOR FIGHTER**

Submitted by **DAVID MUHIRE** in partial fulfillment of the requirements for the degree of **Master of Science in Aerospace Engineering, University of Turkish Aeronautical Association** by,

Assoc. Prof. Dr. Adnan GÜZEL  
Dean, **The School of Graduate Studies, UTAA**

Prof. Dr. Uğur Murat LELOĞLU  
Head of the Department, **Aerospace Engineering, UTAA**

Assoc. Prof. Dr. Ali Ruhşen ÇETE  
Supervisor, **Aerospace Engineering, UTAA**

**Examining Committee Members:**

Assoc. Prof. Dr. Ali Ruhşen ÇETE  
**Aerospace Engineering, UTAA**

Assoc. Prof. Dr. Mecit YAMAN  
**Aerospace Engineering, UTAA**

Assoc. Prof. Dr. Melih YILDIZ  
**Aerospace Engineering, ERCIYES University**

Assoc. Prof. Dr. Reza AGHAZADEH  
**Aerospace Engineering, UTAA**

Ass. Prof. Dr. Onur BAŞ  
**Mechanical Engineering, TED University**

Date 12/08/2024



**I hereby declare that all information in this document has been obtained and presented in accordance with academic rules and ethical conduct. I also declare that, as required by these rules and conduct, I have fully cited and referenced all material and results that are not original to this work.**

David, Muhire

Signature:

## **ABSTRACT**

### **CFD STUDY FOR A TWIN-ENGINE AFTERBODY MODEL INTERCEPTOR FIGHTER**

Muhire, David  
Master of Science, Aerospace Engineering  
Supervisor: Assoc. Prof. Dr. Ali Ruhşen Çete

August 2024, 71 pages

The focus of this thesis is to conduct a thorough analysis comparing computational fluid dynamics (CFD) simulations and experimental data obtained from the Langley Transonic Wind Tunnel. The comparison specifically pertains to the pressure distribution around the nozzle of a twin-engine aircraft afterbody model. The main goal of this study is to assess the precision of CFD simulations by comparing them with empirical data collected under controlled conditions in the wind tunnel.

The approach includes creating a comprehensive 3-DOF twin-engine afterbody design, which includes accurate dimensions as detailed in the paper for the experiments. This representation is then used for conducting CFD simulations at Mach number 0.8 and 0.9, Nozzle Pressure Ratio of 3.4 and at 0 angle of attack, replicating the parameters examined in the Langley Transonic Wind Tunnel.

The pressure distributions around the nozzle are carefully compared, taking into account data from both CFD simulations and wind tunnel experiments, to evaluate the relationship between simulated and real aerodynamic performance. Specific focus is placed on areas of importance such as the nozzle exit plane and the afterbody surface, where intricate flow phenomena like shock waves and boundary layer separation could take place.

The findings of this comparison study provide important information about the trustworthiness of CFD tools in forecasting the aerodynamic performance of twin-engine arrangements at transonic velocities. Discrepancies between the simulated and

observed data are examined to pinpoint possible constraints in the computational models or experimental configurations, resulting in suggestions for future research and development endeavors focused on improving the precision of aerodynamic forecasts for advanced aircraft designs.

**Keywords:** Fighter Jet, Twin-Engine Afterbody, 3-DOF Twin Engine Afterbody, CFD



## ÖZ

### ÇİFT MOTORLU BİR ARKA GÖVDE AVCI SAVAŞ UÇAĞININ HAD ÇALIŞMASI

Muhire, David  
Yüksek Lisans, Havacılık ve Uzay Mühendisliği  
Tez Yöneticisi: Doç.Dr. Ali Ruhşen Çete

Ağustos 2024, 71 sayfa

Bu tezin odak noktası, hesaplamalı akışkanlar dinamiği (CFD) simülasyonları ile Langley Transonik Rüzgar Tüneli'nden elde edilen deneysel verileri karşılaştırarak kapsamlı bir analiz yapmaktır. Karşılaştırma özellikle çift motorlu bir uçağın arka gövde modelinin nozulu etrafındaki basınç dağılımıyla ilgilidir. Bu çalışmanın temel amacı, CFD simülasyonlarının hassasiyetini, rüzgar tüneline kontrollü koşullar altında toplanan ampirik verilerle karşılaştırarak değerlendirmektir.

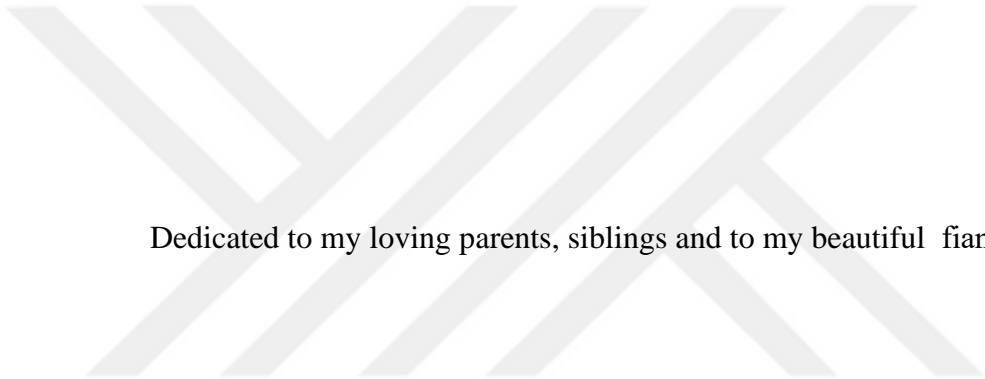
Yaklaşım, deneyler için makalede ayrıntılı olarak belirtildiği gibi doğru boyutları içeren kapsamlı bir 3-DOF çift motorlu arka gövde tasarımının oluşturulmasını içermektedir. Bu gösterim daha sonra 0,8 ve 0,9 Mach sayısında, Nozül Basınç Oranı 3,4'te ve 0 hücum açısında CFD simülasyonlarının gerçekleştirilmesi için Langley Transonik Rüzgar Tüneli'nde incelenen parametrelerin kopyalanması için kullanılır.

Simüle edilmiş ve gerçek aerodinamik performans arasındaki ilişkiyi değerlendirmek için, hem CFD simülasyonlarından hem de rüzgar tüneline deneylerinden elde edilen veriler dikkate alınarak nozül etrafındaki basınç dağılımları dikkatlice karşılaştırılır. Şok dalgaları ve sınır tabakası ayrımı gibi karmaşık akış olaylarının meydana gelebileceği nozül çıkış düzlemi ve gövde sonrası yüzeyi gibi önemli alanlara özel olarak odaklanılır.

Bu karşılaştırma çalışmasının bulguları, transonik hızlarda çift motorlu düzenlemelerin aerodinamik performansını tahmin etmede CFD araçlarının güvenilirliği hakkında önemli bilgiler sağlamaktadır. Simüle edilen ve gözlemlenen veriler arasındaki tutarsızlıklar, hesaplamalı modellerdeki veya deneysel konfigürasyonlardaki olası kısıtlamaları belirlemek için incelenir ve bunun sonucunda, gelişmiş uçak tasarımları için aerodinamik tahminlerin hassasiyetini artırmaya odaklanan gelecekteki araştırma ve geliştirme çabaları için öneriler sunulur.

**Anahtar Kelimeler:** Savaş Jeti, Çift Motorlu Arka Gövde, 3 DOF Çift Motorlu Arka Gövde, CFD





Dedicated to my loving parents, siblings and to my beautiful fiancé

## ACKNOWLEDGMENTS

I would like to convey my heartfelt appreciation and thanks to my supervisor, Assoc. Prof. Dr. Ali Ruşen ÇETE, for providing me with the opportunity for this thrilling study. I am grateful for the extensive office hours he has devoted to me, guiding me through my academic journey and, above all, believing in me until the end. His priceless experience and expertise in conceptual aircraft design have consistently helped me in every step of my progress.

I want to show my sincere appreciation to the other candidates in my Master's program for their unwavering support and camaraderie. Your insights, encouragement, and collaboration have been invaluable throughout this journey. Thank you for being an integral part of my academic experience and for making this journey truly memorable.

Most importantly, my parents, siblings, and friends have my deepest gratitude for their constant support, encouragement and prayers, which have been the beacon of hope throughout this journey. My parents' constant belief in my abilities and their sacrifices have laid the foundation for my success. My siblings have been my pillars of strength, offering their unconditional love and camaraderie in every step i take. My fiancé's love and steadfast faith in me and their continuous motivation have been a source of immense comfort and inspiration. Together, their endless support has empowered me to overcome challenges and pursue my dreams with confidence and determination.

## TABLE OF CONTENTS

ABSTRACT.....	v
ÖZ .....	vii
ACKNOWLEDGMENTS .....	x
TABLE OF CONTENTS .....	xi
LIST OF TABLES .....	xiii
LIST OF FIGURES .....	xiv
LIST OF ABBREVIATIONS .....	xv
LIST OF SYMBOLS .....	xvi
1. INTRODUCTION .....	1
1.1 Review of The Literature.....	5
1.2 Motivation.....	9
1.3 Analysis Comparing Aircrafts that Are Similar.....	10
1.3.1 Introduction .....	10
1.3.2 Arrangements and Responsibilities .....	10
1.3.3 Design parameter comparison .....	13
1.3.4 Analysis and Summary.....	15
1.4 Specifying The Mission .....	15
1.4.1 Description of The Mission .....	16
1.4.2 Flight Profile.....	18
1.4.3 Requirements for The Mission .....	19
1.4.4 Discussion and Conclusion .....	20
1.5 Introduction to Stability .....	21
1.5.1 Static Stability .....	22
1.5.2 Dynamic Stability.....	23
2 METHODOLOGY.....	25
2.1 Geometry Configuration .....	25
2.1.1 Vertical and Horizontal Tails Configuration.....	26
2.1.2 Nose and Body Shape.....	27
2.1.3 Afterbody Configuration .....	27
2.2 Mesh Generation .....	28
2.3 Analysis Using Ansys Fluent.....	30

3	RESULTS AND DISCUSSION .....	35
3.1	Modeling of Conceptual Configuration .....	35
3.2	Simulation (Computational) Details.....	37
3.3	Results of the Study.....	38
3.3.1	Pressure Coefficient (Cp) plots.....	38
3.3.2	Mach Number Plots .....	45
4	CONCLUSION .....	47
4.1.	Overall Conclusion.....	47
4.2.	Future Work.....	48
	REFERENCES.....	50



## LIST OF TABLES

Table 1.1: Similar aircraft arrangements and roles [18][19][20][21][22][23][24][25] .....	12
Table 1.2: Comparison of Aircraft parameters [18][19][20][21][22][23][24][25] .	13
Table 1.3: Mission Specifications and Description [27].	17
Table 4.1: ANSYS Physics setup- <b>General</b> .....	32
Table 4.2: ANSYS Physics setup- <b>Cell Zone and Boundary Conditions</b> .....	33
Table 4.3: ANSYS Physics setup- <b>Solutions</b> .....	34



## LIST OF FIGURES

Figure 1.1: Photograph of the Twin Engine Afterbody model installed in the Langley 16-Foot Transonic Tunnel [8] .....	5
Figure 1.2: Mission Profile for Interceptor Fighter Aircraft [28]. .....	19
Figure 2.1: Wing and tail span dimensions in Solidworks.....	25
Figure 2.2: Dimensions of the VT, HT and the Nozzle. ....	26
Figure 2.3: Lengths of the model from the nose. ....	27
Figure 2.4: Afterbody dimensions in Solidworks. ....	28
Figure 2.5: Mesh of the domain. ....	29
Figure 2.6: Side view of the surface mesh .....	29
Figure 2.7: Front view of the surface mesh.....	30
Figure 2.8: Rear view of the surface mesh.....	30
Figure 3.1: A 3D Sketch view of the twin Engine afterbody Model in Solidworks.....	35
Figure 3.2. Convergent-Divergent Nozzle Geometric Details in cm. ....	36
Figure 3.3: Half body view of a Twin Engine Afterbody model in Fluent featuring a forward vertical and mid horizontal tails. ....	36
Figure 3.4: Circumferential Positions of Pressure Orifice rows for Left and Right Nozzles. ....	38
Figure 3.5: Contour of Pressure Coefficient at $M=0.8$ .....	39
Figure 3.6: Contour of Pressure Coefficient at $M=0.9$ .....	39
Figure 3.7: Contour of Static Pressure at $M = 0.8$ .....	40
Figure 3.8: Contour of Static Pressure at $M = 0.9$ .....	40
Figure 3.9: $C_p$ plots for $M = 0.8$ , $NPR = 3.4$ and $\theta = 180^\circ$ .....	41
Figure 3.10: $C_p$ plots for $M = 0.8$ , $NPR = 3.4$ and $\theta = 225^\circ$ .....	41
Figure 3.11: $C_p$ plots for $M = 0.8$ , $NPR = 3.4$ and $\theta = 240^\circ$ .....	42
Figure 3.12: $C_p$ plots for $M = 0.9$ , $NPR = 3.4$ and $\theta = 180^\circ$ .....	43
Figure 3.13: $C_p$ plots for $M = 0.9$ , $NPR = 3.4$ and $\theta = 225^\circ$ .....	44
Figure 3.14: $C_p$ plots for $M = 0.9$ , $NPR = 3.4$ and $\theta = 240^\circ$ .....	44
Figure 3.15: Mach Number Contour at $M = 0.8$ and $NPR = 3.4$ . ....	46
Figure 3.16: Mach Number Contour at $M = 0.9$ and $NPR = 3.4$ .....	46

## LIST OF ABBREVIATIONS

CFD	Computational Fluid Dynamics
DOF	Degree Of Freedom
A/B	Afterbody
AD	Aircraft Design
NPR	Nozzle Pressure Ratio
AoA	Angle of Attack
AR	Advisory Report
IF	Interceptor Fighter
NASA	National Aeronautics and Space Administration
AGARD	Advisory Group for Aerospace Research and Development
AMT	Advanced Military Trainer
SAS	Stability Augmentation System
BC	Boundary Conditions

## LIST OF SYMBOLS

$W_{TO}$	Take-off weight
$W_E$	Empty weight
$W_F$	Fuel weight
$W/S_g$	Wing loading
$T/Wg$	Thrust-to-weight ratio
$V_{Max}$	Maximum velocity
$S$	Wing Area
$b$	Wing span
$\xi$	Damping ratio
$\alpha$	Angle of attack
$\delta$	Deflection angle of a control surface
$\lambda$	Eigenvalue
$\omega$	Oscillation frequency
$\omega_d$	Damped frequency
$\omega_n$	Natural undamped frequency
$L/D$	Aerodynamic efficiency
$M$	Mach number
$C_p$	Pressure coefficient
$x$	Axial distance
$L$	Length of the aircraft
$x/L$	Normalized axial distance

## CHAPTER 1

### INTRODUCTION

The aviation industry is experiencing a significant surge in research activities related to aircraft design, driven by rapid advancements in modern technology. This field encompasses the development of flying machines tailored to meet specific customer specifications and requirements, encompassing both military and commercial aircraft. Given the intricate geometrical features and demanding maneuver requirements of contemporary tactical aircraft, computational fluid dynamics (CFD) emerges as a viable substitute for traditional experimentation in the realm of conceptual design analysis[1]. Designers and engineers are not only focused on improving existing models but are also pioneering revolutionary new concepts and technologies. These efforts aim to enhance performance, efficiency, and safety, while also addressing emerging demands such as sustainability and environmental impact. The continuous innovation in materials, aerodynamics, propulsion systems, and avionics is propelling the aviation industry towards new horizons, promising more advanced, efficient, and versatile aircraft for various applications.

There are three stages to designing an aircraft, according to [2], [3][4][5], namely;

- **Conceptual design:** This is the first stage in aircraft design. In this stage, designers include sketches of various aircraft configurations as material for consideration to meet the specifications needed such as aerodynamics, propulsion, performance, structure and control. The fundamental aspects like the wing configuration, engine size and fuselage shape are established at this stage. At this stage, all the aforementioned design constraints are also considered. The final product of conceptual design is the guesswork of a sketch in the form of a plane configuration layout concept.

- Preliminary design: The subsequent stage of the design process involves the revisions and modelling of the design in the form of parameters. During this stage, the model undergoes aerodynamic testing which is conducted using wind tunnels and CFD. Additionally, comprehensive analyses are performed to evaluate the structure and control aspects. The final result of the preliminary design stage encompasses improved sketches along with the dimensions of the aircraft's geometry and parameters.
- Detail design: At this stage in the process, the design should be prepared for the transition to manufacturing stage. For instance, during the conceptual and preliminary design stages, designers typically focus on creating a general geometric representation of the wings. However, during the detailed design stage, designers must elaborate on the wing designs by breaking them down into components such as ribs, spars and skins, each of which necessitates individual design and analysis. Additionally, an essential aspect at this stage is production design. A specialist must possess the capability to outline the manufacturing process of the aircraft, starting from the preparation of subassemblies to the final assembly. Designers must also establish the most straightforward, cost-effective and efficient manufacturing procedures at this stage.

The initial stage of aircraft design involves defining the concept, a highly creative and imaginative phase where the connectivity and geometry placement, and of the components of a future airplane are determined to meet the requirements of a particular market. During this stage, engineers and designers explore various innovative ideas and configurations, focusing on how each component interacts and contributes to the overall performance of the aircraft. This involves brainstorming and developing multiple concepts that push the boundaries of conventional design. The goal is to envision a new aircraft that meets specific performance criteria, such as speed, range, and payload capacity, while also considering factors like manufacturability and maintainability. This stage is crucial for setting the foundation of the aircraft's design, ensuring that it aligns with market demands and operational needs.

The conceptual design process also involves a rigorous evaluation of the new aircraft concept against more conventional layouts at a system-wide level. This comparative analysis helps in identifying the most promising configuration that offers technical advancements and economic viability. Engineers use advanced modeling and simulation tools to assess various design options, considering factors such as aerodynamics, structural integrity, propulsion efficiency, and cost-effectiveness. The objective is to identify a preferred configuration that not only incorporates cutting-edge technology but also remains feasible within the constraints of budget and production capabilities. By balancing innovation with practicality, the conceptual design stage aims to create a blueprint for an aircraft that stands out in the competitive market, offering superior performance and efficiency while meeting the anticipated needs of future users [3].

In accordance with the purpose, the main tasks of fighter-interceptors are;

- Destruction of aviation cruise missiles
- Destruction of enemy airborne assault forces in the air
- Destruction of long-range radar detection aircraft,
- Jamming aircraft and bombers
- Support for combat operations of units of other types of aviation
- Destruction of land and sea objects

In the field of aerospace engineering, creating cutting-edge military aircraft like the twin-engine afterbody model interceptor fighter requires a comprehensive understanding of its aerodynamic properties, particularly concerning longitudinal dynamic stability [6]. This aspect of stability is crucial for maintaining the aircraft's balance and control during various flight maneuvers [7]. The objective of this research is to investigate the complex interactions that contribute to the long-term stability of the twin-engine afterbody model interceptor fighter. This investigation focuses on how its aerodynamic design, propulsion systems, and control mechanisms work synergistically to influence stability. By thoroughly examining current literature and utilizing advanced computational simulations, the study aims to identify and analyze

the critical elements that impact the longitudinal stability of these high-performance aircraft.

Computational methods provide substantial advantages over traditional experimental approaches when addressing aerodynamic engineering problems. Replicating an entire system for wind tunnel testing is often impractical due to the high costs, time requirements, and logistical challenges involved. Constructing physical models to scale and setting up wind tunnel experiments can be prohibitively expensive and labor-intensive, making it difficult to explore a wide range of design modifications quickly. In contrast, numerical methods, such as Computational Fluid Dynamics (CFD), enable engineers to simulate and analyze aerodynamic performance with high precision and flexibility. These simulations allow for rapid iteration and optimization of designs, facilitating the exploration of numerous configurations and parameters without the need for physical prototypes. Consequently, numerical aerodynamic analyses have become indispensable in the design process, significantly enhancing the efficiency and effectiveness of both conceptual and detailed design stages.

The importance of developing a robust solver capable of accurately and swiftly modeling aerodynamic analyses for complex geometric structures cannot be overstated. Such a solver must integrate advanced algorithms and high-performance computing resources to handle the intricate details and interactions within aerodynamic flows. Accurate numerical simulations are essential for predicting critical performance metrics, such as lift, drag, and stability, which are vital for the successful design of aircraft and other aerodynamic vehicles. Moreover, a well-developed solver can facilitate the early identification of potential issues, enabling engineers to make informed decisions and implement necessary modifications during the design process. This proactive approach reduces the risk of costly redesigns and ensures that the final product meets the desired performance criteria.

In summary, the advancement of computational methods and the development of sophisticated solvers are pivotal in driving innovation and efficiency in aerodynamic engineering, ultimately leading to more advanced, reliable, and cost-effective aerospace designs.

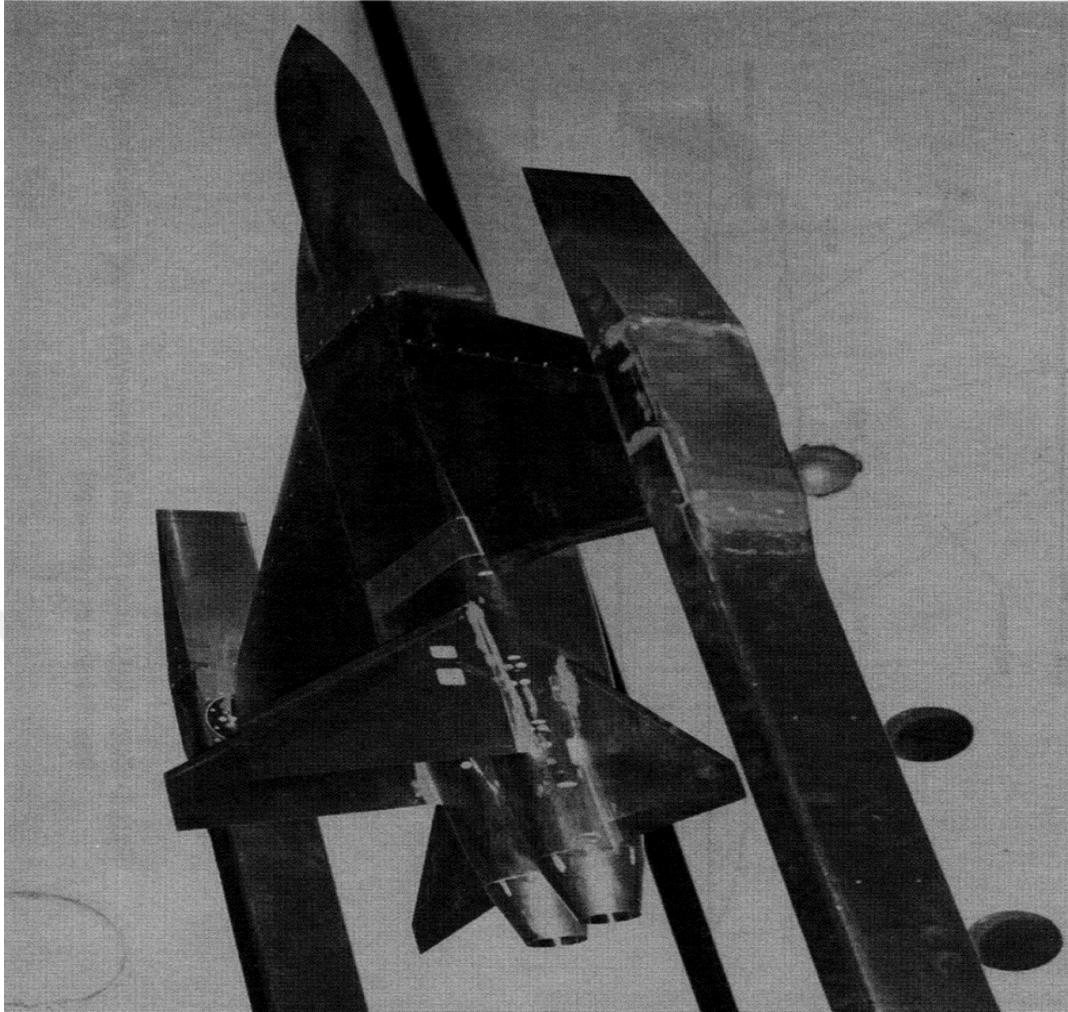


Figure 1.1: Photograph of the Twin Engine Afterbody model installed in the Langley 16-Foot Transonic Tunnel [8]

## 1.1 Review of The Literature.

There has been limited research on the design of fighter aircraft because they are primarily used for military purposes, which restricts access to comprehensive aeronautical information about these aircraft. Following is a summary of the reviewed related works.

In his paper, David J. Wing conducted a wind tunnel test to examine how various empennage and afterbody factors impact the aerodynamic features at the rear-end of a twin-engine fighter-type aircraft.[8]

A project presented focused on 3-DOF longitudinal flight simulation modeling using Matlab/Simulink. An elementary 3-DOF longitudinal flight simulation model has been constructed for examining aircraft behavior. The designer would have the ability to predict how the aircraft would perform in particular flight scenarios and is able to develop a stable and manageable airplane by analyzing its characteristics of stability. Employing testing based on simulation prior to carrying out real flight experiments would result in saving both time and resources. The query arises concerning the applicability of the simulation model for a designer looking to create an innovative aircraft design and wishing to explore fundamental airplane dynamics.[9]

A paper [10] presented focused on the Afterbody/Nozzle pressure distributions of a twin-tail twin-engine fighter with axisymmetric nozzles at Mach numbers from 0.6 to 1.2. The Langley 16-Foot transonic tunnel was utilized to acquire the static pressure coefficient distributions over the afterbody and axisymmetric nozzles of a standard twin-tail twin-engine fighter aircraft. A comprehensive investigation was conducted involving three different longitudinal positions for the vertical tail and two longitudinal positions for the horizontal tail, resulting in a number of 6 rear-end settings. The  $c_p$  was measured at various conditions including M of 0.6, 0.8, 0.9 and 1.2, attack angles of  $0^\circ$ ,  $4^\circ$  and  $8^\circ$ , and ratios of nozzle pressure starting from jet-off to 8. The measurement of pressure was done at nearly 150 areas encompassing the A/B, interfairing regions and nozzles. The findings from this study indicate that the influence of the vertical and horizontal tails extends beyond the region adjacent to the tail-afterbody junction<sup>1</sup>. In summary, the distribution of pressure that affects drag at the rear section of the aircraft is more significantly influenced by the positioning of the vertical stabilizers compared to that of the horizontal stabilizers.[10]

A study was performed in the Langley 16-Foot Transonic Tunnel to investigate how various empennage and A/B characteristics affect the aerodynamic properties of the rear-end of a fighter plane with twin-engine. The variables of the model included the axial location of HT and incidence, the axial positioning of the VT, along with its configuration—whether twin or single-tail, tail booms and the adjustments of the nozzle power settings. Testing was done at angles of attack between  $-20^\circ$  and  $10^\circ$ , jet total pressure ratios between jet-off conditions and about 10, and Mach numbers

between 0.6 and 1.2. The findings obtained from this study indicated that the influence of tail interference effects was apparent throughout the full range of Mach numbers that were examined. These effects accounted for a significant portion of the total drag experienced at the aft-end during transonic speeds. Notably, the influence of tail interference on the nozzles was predominantly negative, with the severity of these effects appearing to escalate as the empennage surfaces were situated nearer to the nozzles. [11].

The conceptual design of a twin-engine afterbody model interceptor aircraft hinges on the establishment of clear mission requirements. These requirements are instrumental in driving the process of the design and determining the performance of the airplane. Requirements of the mission are drawn from available studies on similar aircraft types and customer specifications. Engineers and designers are faced with the challenges of addressing these requirements as problems that need to be solved. According to Kamal et al, problem formulation methods are employed, which involve using benchmarks, defining problems, assessing their significance, generating concepts, selecting and evaluating configurations [12].

In a study, the writers investigated the potential impact of a specific trend in wingspan on the dynamic stability of aircraft and also evaluated the response of controlling flaps positioned on both the front and rear wings. Using MGAERO software, the CFD computations yielded the essential aerodynamic data and control derivatives. The equations governing the longitudinal motion of the aircraft were formulated in a state space form incorporating the aerodynamic coefficients, stability and control derivatives. The investigation of dynamic stability was conducted in Matlab by solving the eigenvalue problem, whereas the evaluation of the system's response to control inputs was carried out using the step response method within the Matlab framework. The findings of this analysis demonstrated a nonlinear relationship between wing size and aircraft dynamic stability characteristics, primarily due to a strong aerodynamic coupling. Noteworthy is the increased oscillation observed with the front flap in cases of flap deflection [13].

A research paper presents a computational investigation that explores the airflow around an airplane at practical velocities. It underscores the importance of broadening

the current analysis to encompass the entire aircraft, stressing its crucial contribution to improving the performance of the airplane during flight. Utilizing ANSYS Fluent (19.2) software, a comprehensive study was conducted on the F16 and F22 aircraft and the purpose was to determine the shear stress distribution and temperature variation and pressure distribution across the entire surface of the aircraft. A comprehensive examination of the results across the entire surface indicates that F16 encounters reduced pressure levels, specifically 29% and 30% lower at Mach 1 and Mach 2, respectively. Additionally, the temperature is also diminished, showing reductions of 9.5% at Mach 1 and 30% at Mach 2, and shear stress (90% and 83% lower for Mach 1 and Mach 2 respectively) in comparison to F22. Overall, the performance of an aircraft is heavily dependent on its design [14].

In August 2018, a project aimed at conceptualizing an aircraft design was initiated, guided by the specifications of the T-X program for an advanced military trainer (AMT). The design phase encompassed various critical elements, including the selection of configurations, weight and performance sizing, as well as the design of the fuselage, wings, empennage, and landing gear. Additionally, considerations for weight and balance, static longitudinal and directional stability, and drag polars were integral to the process. Following this initial conceptualization, the design was further refined through Class II methodologies, which encompassed techniques such as supersonic area ruling, approximations of drag polars, V-n diagrams, Class II evaluations of weight and balance, calculations of moments and products of inertia, as well as estimations of costs. [15].

In their study, Defne KIRAN and Ali Ruşen ÇETE developed a multiblock structured grid solver for solving the 3D Euler/Navier-Stokes equations. The algorithm utilizes the finite difference method in conjunction with the lower-upper factorization technique to deliver rapid solutions. Additionally, the incorporation of multiblock structured grids enhances its applicability to intricate geometric configurations. Subsequently, the newly developed solver is evaluated using a "body-only" axisymmetric model that includes the rear-end of a single-engine fighter, a setting that had been previously studied through experimental means. The solver's numerical analysis of pressure distributions on the model's body was compared with experimental

data, revealing a strong agreement between the two sets of results. They concluded that the solver effectively solves the flow equations and accurately represents the flow's physical characteristics[16].

## **1.2 Motivation**

The evolution of sophisticated interceptor aircraft is motivated by numerous crucial elements that influence contemporary aerial warfare and defense tactics. Twin-engine interceptors possess the capability to effectively engage in diverse combat scenarios, ranging from engagements at high altitudes to interceptions at low levels.

This adaptability plays a vital role for modern air forces that necessitate multi-role capabilities. The operational range of the aircraft is enhanced by the presence of two engines, allowing for a greater fuel capacity. This becomes especially crucial when dealing with potential threats located at a considerable distance from the home base or when conducting surveillance over a vast airspaces.

Twin-engine interceptors possess the ability to extend their power and influence across a broader expanse, thereby providing support for defensive as well as offensive endeavors. This particular capability plays a pivotal role in upholding air superiority within regions that are fiercely contested. As adversaries continue to enhance their aircraft and missile systems, it becomes imperative to have interceptor fighters that can not only keep up with but also surpass these advancements and twin-engine designs offer necessary performance and capabilities to effectively counter these evolving threats.

The motivation behind the development of a twin-engine afterbody model interceptor fighter lies in the desire to improve performance, operational flexibility, reliability, technological integration, strategic advantage and the capacity to address new challenges. This particular design seeks to offer a resilient and adaptable platform that can uphold air dominance and safeguard national interests amidst a rapidly evolving and intricate global environment.

### **1.3 Analysis Comparing Aircrafts that Are Similar.**

#### **1.3.1 Introduction**

Military fighter aircrafts are considered to be highly intricate technological advancements within the field of aviation. These aircrafts play a crucial role in military strategies, serving multiple purposes. Their primary objective is to ensure the safety and security of the airspace. Specifically designed for air superiority, these aircrafts possess the capability to effortlessly dominate the airspace through swift interception, engaging in air-to-air combat and providing support when required.

In the study on similar aircraft, a lot of aircrafts were subjected to review. Among them, eight specific aircrafts were chosen for the purpose of this design. These eight aircrafts are namely the F-14 Tomcat, F-15 Eagle, Panavia Tornado, Su-15 Flagon, Mig-29 Fulcrum, Mig-31 Foxhound, F-22 Raptor and F/A-18 Super Hornet. The F-14, developed by the United States in 1974, is a long-range air superiority aircraft that possess multiple roles including interception, aerial engagement and airborne surveillance. The primary interest in this aircraft revolved around its wings with adjustable sweep angle, main plane arrangements and size. As for the F-15, its ability to cover distances, top speed, and setup options seemed to be highly favorable parameters to incorporate into the design. The Su-15, on the other hand, is a an interceptor developed by the Soviet Union in 1965. The investigation focused on examining the similarities in terms of payload, armaments and dimensions. The design considerations also took into account Mig's maximum altitude at which it can operate effectively, its ability to engage in aerial combat, the highest attainable velocity, and the weapons it carries.

#### **1.3.2 Arrangements and Responsibilities**

These aircrafts were constructed with distinct missions and functions in mind. To effectively carry out their designated tasks, every airplane was to be customized in order to have the specific criteria that the designers established. The settings detailed

in the following table encompassed elements such as wing structure, propulsion system, tail design and crew composition. The majority of these aircrafts featured similar configurations. Furthermore, a comparative analysis of these aircrafts was conducted to explore their individual roles. With the exception of Su-15, all of these aircrafts were categorized as air superiority fighters.

These aircraft were primarily designed to assert control[17] over the airspace through their advanced capabilities in aerial engagement, intercept mission and supporting on the ground. In aerial engagement, the design focuses on achieving superior maneuverability, speed, and advanced avionics to outmaneuver and engage enemy aircraft effectively. For interception missions, the aircraft are equipped with powerful engines and sophisticated radar systems to detect, track, and neutralize incoming threats swiftly. Ground support roles necessitate robust structural integrity, precision targeting systems, and the ability to carry a diverse array of munitions for close air support and strategic strikes. Integrating these multifaceted capabilities requires a meticulous balance of aerodynamics, propulsion, avionics, and weapons systems, ensuring the aircraft can perform efficiently across different mission profiles while maintaining high levels of survivability and operational effectiveness in contested environments.

**Table1.1:** Similar aircraft arrangements and roles [18][19][20][21][22][23][24][25]

<b>Name</b>	<b>Configuration</b>	<b>Roles</b>
F-14(1970)	<ul style="list-style-type: none"> <li>❖ Adjustable sweep wing</li> <li>❖ Conventional tail</li> <li>❖ 2-engines</li> <li>❖ 2 crew</li> </ul>	<ul style="list-style-type: none"> <li>❖ Air superiority</li> <li>❖ Interceptor</li> <li>❖ Multirole</li> </ul>
F-15(1976)	<ul style="list-style-type: none"> <li>❖ Swept wing</li> <li>❖ Conventional tail</li> <li>❖ 2 engines</li> <li>❖ 1 crew</li> </ul>	<ul style="list-style-type: none"> <li>❖ Air superiority</li> <li>❖ Double role</li> </ul>
Panavia Tornado (1979)	<ul style="list-style-type: none"> <li>❖ Variable sweep wing</li> <li>❖ Conventional tail</li> <li>❖ 2 engines</li> <li>❖ 2 crew</li> </ul>	<ul style="list-style-type: none"> <li>❖ Interceptor</li> <li>❖ Multirole</li> </ul>
Su-15 (1965)	<ul style="list-style-type: none"> <li>❖ Trapezoidal wing</li> <li>❖ Conventional tail</li> <li>❖ 2 engines</li> <li>❖ 1 crew</li> </ul>	<ul style="list-style-type: none"> <li>❖ Interceptor</li> </ul>
Mig-29 (1997)	<ul style="list-style-type: none"> <li>❖ Swept wing</li> <li>❖ Conventional tail</li> <li>❖ 2 engines</li> <li>❖ 1 crew</li> </ul>	<ul style="list-style-type: none"> <li>❖ Air superiority</li> <li>❖ Multirole</li> </ul>
Mig-31 (1979)	<ul style="list-style-type: none"> <li>❖ Swept wing</li> <li>❖ Conventional tail</li> <li>❖ 2 engines</li> <li>❖ 2 crew</li> </ul>	<ul style="list-style-type: none"> <li>❖ Interceptor</li> </ul>
F-22(2005)	<ul style="list-style-type: none"> <li>❖ Swept wing</li> <li>❖ Conventional tail</li> <li>❖ 2 engines</li> <li>❖ 1 crew</li> </ul>	<ul style="list-style-type: none"> <li>❖ Air superiority</li> <li>❖ Multirole</li> </ul>
F/A-18 (1983)	<ul style="list-style-type: none"> <li>❖ Swept wing</li> <li>❖ Conventional tail</li> <li>❖ 2 engines</li> <li>❖ 1 crew</li> </ul>	<ul style="list-style-type: none"> <li>❖ Multirole</li> </ul>

### 1.3.3 Design parameter comparison

A wide range of parameters influences the design of an aircraft, making the process inherently complex and multidisciplinary. In the investigation of chosen aircraft, key design characteristics like weight, loading of the wing, aspect ratio, payload, and ratio of thrust-to-weight were meticulously reviewed. Weight considerations are crucial for determining the aircraft's performance and structural integrity. Wing loading affects lift and maneuverability, while the aspect ratio influences aerodynamic efficiency and drag. Payload capacity is vital for defining the aircraft's operational utility, and the thrust-to-weight ratio directly impacts acceleration and climb performance. The interaction among these parameters necessitates a balanced approach, as adjustments in one area often lead to significant effects in others. This interconnectedness demands a comprehensive understanding of aerodynamics, materials science, propulsion, and systems engineering to achieve an optimal design that meets performance, safety, and economic requirements.

**Table 1.2:** Comparison of Aircraft parameters [18][19][20][21][22][23][24][25]

Parameter	Units	F-14	F-15	Panavia Tornado	Su-15
$W_{TO}$	lb	70,345	44,500	61,700	37,920
$W_E$	lb	39,930	28,700	32,000	23,973
$W_F$	lb	24,912	36,200		12,345
$W/S_g$	lb/ft <sup>2</sup>	124.5	73.2		96
Thrust(dry)/ (afterburner)	lbf	25,000	17,800/ 29,100	9,104/ 16,410	18,682
$T/W_g$	-	0.57	1.07		0.49
TSFC (dry/ Afterburner)	lb/h*lbf	0.88/2.26	0.76/1.94		0.93/2.209
Range	nmi	1,620.8	2,088.7	1,150	961
$V_{Max}$	mph	1,584	1,676	1,452	1,386
Rate of Climb	feet/ min	45,000	50,000	40,000	45,000

**Table 1.3 (Continue):** Comparison of Aircraft parameters  
 [18][19][20][21][22][23][24][25]

Parameter	Units	F-14	F-15	Panavia Tornado	Su-15
Service Ceiling	ft	50,000	65,000	50,000	60,000
S	ft <sup>2</sup>	565	608	286	394
b	ft	64.1/37.6	42.8	45,8	30.7
AR	-	7.3/2.5	3.01		-
Length	ft	62.7	63.8	61,3	67.42
Payload	lb	5,687	4,800	3,915	3,086
W <sub>TO</sub>	lb	37,037	80,953	83,500	51,900
W <sub>E</sub>	lb	24,030	48,100	43,340	23,000
W <sub>F</sub>	lb	8,818	31,305	26,000	10,860
W/S <sub>g</sub>	lb/ft <sup>2</sup>	90.5	122.5	77.2	93
Thrust(dry)/ (afterburner)	lbf	22,302	41,814	26,000/ 35,000	
T/W <sub>g</sub>	-	1.09	0.85	1.08	0.96
TSFC (dry/ Afterburner)	lb/h*lbf	0.77/2.05	0.72/1.86		
Range	nmi	802.6	1,620.8	1,738	1,089
V <sub>Max</sub>	mph	1,532	1,864	1,600	1,190
Rate of Climb	feet/ min	65,000	41,000	62,000	50,000
Service Ceiling	feet	59,000	67,651	65,000	40,000
S	ft <sup>2</sup>	409	663	840	410
b	ft	37.3	44	44.6	44.1
AR	-	3.4	2.94	2.36	4
Length	ft	56.8	74.2	62,1	56.1
Payload	lb	10,582	22,429	29,410	

### **1.3.4 Analysis and Summary**

The comparative analysis of eight aircrafts revealed that each aircraft possesses distinct parameters. Notably, five of them were designed to be operated by one crew member. Nevertheless, this particular configuration did not have a substantial impact on the overall length of the aircraft, as most of them were of similar sizes. The aircrafts predominantly featured propulsion systems with two engines, with a majority of them being turbofan engines fitted with afterburners.

Furthermore, analysis of performance parameters revealed that all aircrafts had extraordinarily high climb rates of more than 50,000 feet per minute. The biggest distinction among the eight aircrafts was their payload capacity. The Russian aircrafts appeared to have the most payload capacity, weighing in excess of 10,000 pounds. Despite being the lighter of the two aircraft, the MIG-29 was nonetheless able to transport such heavy payload. Furthermore, the wing loading amongst the eight aircrafts differed. The F-15 exhibited the least loading of the wing, whereas the MIG-31 possessed the largest area of the wing.

Concluding, it was seen that the ideal aircraft to evaluate for the design similarities was Mig-31. The Mig-31 has the highest maximum velocity, service ceiling and payload of all the eight aircrafts considered.

## **1.4 Specifying The Mission**

Fighter aircraft are required to adhere to stringent mission specifications, including factors such as endurance, the type and weight of ammunition carried, and the cruise Mach number. Consequently, it is essential to accurately estimate both the minimum weight of the aircraft and the fuel weight necessary to achieve the desired flight profile [26]. The intercept mission is a strategic operation performed to reach a combat area as swiftly as possible, aiming to engage and neutralize enemy air vehicles. This mission is crucial in air defense, as it seeks to destroy assigned targets or force them to abort their mission, thereby protecting friendly territories and assets. The key to a successful intercept mission lies in speed, precision, and timing. Interceptor aircraft, specifically

designed for this role, are dispatched to intercept incoming threats, typically bombers and reconnaissance aircraft, which pose significant risks to national security. These missions require rapid response times and precise execution to effectively counter enemy advancements and mitigate potential damage.

Interceptor aircraft are a specialized type of fighter aircraft engineered for the defensive interception role. They are designed to possess long-range capabilities, allowing them to cover vast distances quickly to reach their targets. High speed is another critical characteristic, enabling these aircraft to outpace enemy bombers and reconnaissance planes. Additionally, they are built to operate at high altitudes, which is advantageous for intercepting enemy aircraft that often fly at considerable heights. The combination of these features makes interceptors highly effective in their role, ensuring they can meet and engage enemy threats promptly and efficiently, thereby maintaining air superiority and safeguarding national airspace.

#### **1.4.1 Description of The Mission**

Fighter aircraft serve as the backbone of air forces worldwide, designed primarily for achieving and upholding aerial dominance through air-to-air combat over the battlefield. Their mission encompasses securing control of essential airspace by engaging and destroying enemy aircraft, either fighters of equal capability or bombers equipped with defensive weaponry. To fulfill this role effectively, fighter aircraft must possess exceptional performance characteristics, including high speed, maneuverability, and firepower, enabling them to outfly and outmaneuver opponents.

The aircraft's mission is dependent on the above eight fighter capabilities most especially considering the ones that are still in service like Mig-31, Mig-29, F-15 and F-22.

**Table 1.4:** Mission Specifications and Description [27].

<b>Payload:</b>	The cannons are 20 millimeters and are equipped with 1,000 pounds of weapons ( $W_E$ includes the 250-pound weight of cannon as one of its parts). Carrying 4 80 pounds short, 4 500 pound medium and 2 1,000 pounds Extended range aerial missiles. Weapons are dropped depending on the mission.
<b>Crew:</b>	1 pilot (maximum 250 pounds)
<b>Range and Altitude:</b>	See profile of the mission.
<b>Cruise Speed</b>	500 knots at 15,000 feet Mach = 2.2 (50,000 feet). Mach = 1.4 (47,000 feet).
<b>Climb</b>	Climb gradient > 250 feet/nmi. Supersonic climb (45,000 feet to 50,000 feet). Rate of climb on single engine with maximum $W_{TO}$ > 500 feet/min.
<b>Take-off and Landing:</b>	Ground run < 2,500 feet at sea level. Length of the field for take-off < 3,000 feet and < 5,000 feet for landing. All at sea level
<b>Service Ceiling:</b>	50,000 feet. The combat ceiling: Subsonic conditions = 500 feet/minute maximum. Supersonic conditions = 1,000 feet/minute maximum. The Cruise ceiling: Subsonic conditions = 300 feet/minute maximum. Supersonic conditions = 1,000 feet/minute maximum.
<b>Maneuverability</b>	Rate of turn > $12^0$ / sec with less than 4,500 feet radius of turn at 15,000 feet. 7 GS, velocity of 590 knots at 15,000 feet.
<b>Certification Base:</b>	Military

## 1.4.2 Flight Profile

The concept of mission profile in general aviation pertains to the flight performance of an aircraft as it transitions from one position to another. This mission profile is typically represented as a visual diagram comprising various lines and curves, which serve to depict the diverse specifications and movements associated with different types of aircraft. These diagrams provide a comprehensive overview of the aircraft's capabilities and performance throughout its flight, from takeoff to landing, including aspects such as speed, altitude, and fuel consumption[4]. Understanding the mission profile is essential for pilots and engineers, as it allows them to optimize the aircraft's performance and ensure it meets the specific demands of its intended operational environment.

The term "mission profile" also describes the main purpose or task that a specific type of aircraft is designed to fulfill during its journey. For instance, an interceptor aircraft has a mission profile that is vastly different from that of a commercial aircraft. While interceptors are designed for rapid response, high speed, and high-altitude operations to engage enemy threats, commercial aircraft focus on efficiency, passenger comfort, and long-range capabilities. Consequently, the aircraft's mission profile during the design stages should align with the requirements of its designated role, ensuring that every aspect of its performance, from aerodynamics to fuel efficiency, is tailored to fulfill its specific operational objectives. This alignment is crucial for the successful execution of the aircraft's primary function and overall mission.

To ensure the effective design of an aircraft, it is essential that the mission profile is clear and concise. A mission profile that is overly complicated can result in confusion and misinterpretation during the initial stages of conceptual design. The mission profile for the Interceptor fighter aircraft includes details of performance specifications or segments, including takeoff, climb, cruise range, landing, combat and descent.

	SEGMENT	FUEL	TIME	DISTANCE	SPEED	ALTITUDE	THRUST SETTING <sup>(1)</sup>
A	WARM-UP, TAKEOFF, AND ACCELERATE TO CLIMB SPEED	20 MIN @ GROUND IDLE + 30 SEC @ TAKEOFF / MAXIMUM / RT (A/B IF REQUIRED). NO DISTANCE CREDIT.					
B	ACCELERATE				OBSTACLE CLEARANCE TO 0.9 MACH	TAKEOFF	MAXIMUM/MAXIMUM A/B
C	CLIMB (PARA 4.2.3)				0.9 MACH	TAKEOFF TO 40,000 FEET PRESS ALT.	MAXIMUM/MAXIMUM A/B
D	CRUISE				1.4 MACH OR V <sub>MAX</sub> A/B WHICHEVER IS LOWER. (3)	40,000 FEET PRESS ALT.	
E	COMBAT (2)	ONE 180 DEG TURN @ 1.2 MACH WITH MAX SUSTAINED G's @ MAXIMUM A/B. EXPEND HALF OF AMMO AND MISSILES. NO DISTANCE CREDIT.					
F	CLIMB (PARA 4.2.3)				MINIMUM TIME CLIMB SCHEDULE (4)	40,000 FEET PRESS ALT. TO OPTIMUM CRUISE	INTERMEDIATE
G	CRUISE (PARA 4.2.3)				OPTIMUM CRUISE	OPTIMUM CRUISE	
H	DESCENT (PARA 4.2.3)	NONE	NONE	NO CREDIT		END CRUISE TO LANDING	
I	RESERVES	20 MIN + 5% OF INITIAL FUEL		NO CREDIT	MAXIMUM ENDURANCE	SEA LEVEL	
J							
K							
L							

NOTES: (1) THRUST SETTINGS ARE NON-AUGMENTED/AUGMENTED. (SEE PARA 3.11.3.2) (4) CLIMB SCHEDULE ENDS AT OPTIMUM CRUISE SPEED/ALTITUDE.  
(2) SEE PARA 4.1.5 AND 4.1.7.  
(3) INCLUDE ACCELERATION FUEL TO THE PROPER SPEED.

**Figure 1.2:** Mission Profile for Interceptor Fighter Aircraft [28].

### 1.4.3 Requirements for The Mission

The specifications of the mission serve as the primary influences in the design of contemporary aircraft. The specific configurational characteristics are dictated by the mission requirements, which subsequently influence the extent of the aircraft's attributes. [29]. Developing the mission requirements can be a challenging endeavor, as it is frequently hard to anticipate the future needs and desires.

The determination of mission requirements for interceptor aircraft is made by the specific branch of the military that intends to deploy them. This process involves a thorough assessment of the strategic and tactical needs of the military, considering factors such as the potential threat environment, the types of enemy aircraft expected to be encountered, and the geographical areas where operations will take place. Military planners and defense experts collaborate to define the essential capabilities that interceptor aircraft must possess, such as speed, range, altitude, and armament.

These requirements are then used to guide the design, development, and procurement of interceptor aircraft, ensuring they are equipped to effectively counter threats and fulfill their defensive roles in protecting national airspace and responding to enemy incursions. Multi-role aircrafts or aircraft capable of executing a diverse range of missions can often be quite attractive. These robust aircrafts are designed for their most

challenging missions, which means they are over designed for the other missions. Alongside the mission requirements, it is essential to adhere to particular military specifications.

#### **1.4.4 Discussion and Conclusion**

The criteria and prerequisites for the design of the aircraft were well-suited to those of any interceptor fighter aircraft, aligning closely with the parameters of the aircrafts investigated. These designs ensured that the aircraft possessed the necessary payload capacity and performance characteristics to fulfill its intended roles. Specifically, the aircraft was equipped to excel in air-to-air combat with advanced armaments, allowing it to effectively engage enemy aircraft. Additionally, it was capable of carrying out weapons drop missions, thanks to its sufficient payload capacity and robust delivery systems. The design also included features to support ground operations, such as precision targeting and versatile munitions. This comprehensive capability ensures that the aircraft can perform effectively across a range of mission profiles, providing a balance between combat effectiveness and operational flexibility.

Concluding, mission profile comprehensively details every mission stage, underscoring the necessity for an Interceptor fighter airplane to be adept at handling diverse operational stages. This profile offers an insightful visual representation, illustrating crucial aspects such as the aircraft's speed, operational altitudes, and range capabilities. Additionally, it outlines various combat mission scenarios that the aircraft must be equipped to manage, emphasizing the importance of versatility and adaptability in the aircraft's design to effectively perform throughout the entire mission profile.

## 1.5 Introduction to Stability

The subject of stability holds immense significance when it comes to the design, control and operation of aircraft and other airborne vehicles. It is a critical aspect that must be carefully considered based on the specific type of aircraft under investigation. Commercial aircrafts for instance, prioritize higher stability compared to fighter aircrafts and the reason being that fighter aircrafts need to swiftly execute maneuvers in accordance with their specific purpose.

Stability is the natural tendency of an aircraft to return to its equilibrium position after having any disturbance. These disturbances may be due to atmospheric events like turbulence or flight control inputs like pilot's actions. Therefore, it is of utmost importance to ensure the stability of an aircraft is maintained after encountering any disturbances[30][31].

The pilot's manual commands can provide stability, but this method is not entirely safe or sufficient. It would be challenging and tiring for the pilot to continuously maintain the aircraft's stability after any disturbances. Therefore, aircraft must be equipped with an automatic control system to facilitate the stabilization process. Flight control systems, such as the Stability Augmentation System (SAS), are installed in aircraft to actuate the flight controls and provide the necessary damping to counter disturbances.

Ensuring stability control is crucial for optimal aircraft performance. Inadequate stability control can lead to subpar handling characteristics, posing risks to the safety of both the pilot and the aircraft. Even if an aircraft is flawlessly designed, achieving good flight performance hinges on effective stability control. Therefore, thorough studies on stability and control are essential for achieving superior handling in all flight conditions and optimizing the design of control systems for peak aircraft performance.

Aircraft stability can be divided into two main categories: **Static stability** and **Dynamic stability**.

### **1.5.1 Static Stability**

As discussed above, stability is the natural tendency of an aircraft to return to its equilibrium position after having any disturbance. Thus, static stability can be defined as the ability of an aircraft to revert to its initial flight state after encountering a disturbance or deviation from its intended path. When an airplane experiences a disruption, like a burst of wind or a control maneuver, it will suddenly change its direction. Nevertheless, because of its static stability, the airplane will instinctively move back towards its original position without needing additional control inputs from the pilot [32].

Static stability can be categorized into three types: Positive, neutral and Negative static stability.

An airplane with positive static stability will naturally return to its original altitude after experiencing turbulence. For example, if an aircraft encounters turbulence at a certain altitude, causing its nose to pitch up, the automatic control systems will work to lower the nose and return the aircraft to its original altitude.

The state of neutral static stability occurs when an aircraft, once disturbed from its initial position, neither returns to that position nor strays further from it. Put simply, the aircraft remains in its new position without any inclination to self-correct or alter its trajectory. For example, if an aircraft encounters turbulence at a certain altitude, causing its nose to pitch up, the aircraft will remain in that position through out the flight.

An aircraft with negative static stability tends to continue moving away from its original altitude after experiencing a disturbance. For instance, if an aircraft encounters turbulence and the nose tilts upward, it will continue to move away and pitch up. The condition is typically not preferred for the majority of aircraft, as it has the potential to cause challenges in controlling the aircraft and may result in hazardous situations if not addressed promptly.

### 1.5.2 Dynamic Stability

The dynamic stability of an aircraft relates to its reaction to disturbances over time. This specifically involves examining how the aircraft's behavior changes as it tries to reestablish its equilibrium state after being displaced from it [30], [31], [33]. When an airplane encounters an interruption, like turbulence or a sudden burst of wind, its ability to react and recover its original flight path quickly depends on its dynamic stability.

The immediate response of an aircraft to a disturbance is called short-term dynamic stability, which encompasses any oscillations or deviations from the intended flight path. However, the concept of dynamic stability extends further than the immediate response, also involving the aircraft's behavior over time. This is referred to as long-term dynamic stability.

Dynamic stability can be categorized into three types: positive, neutral and negative dynamic stability.

Aircraft that have positive dynamic stability display oscillations that slowly reduce over time, causing the aircraft to ultimately revert to its initial state. The Cessna 172 is an example of this situation. When the aircraft is trimmed for level flight and then disrupted, it will oscillate around its initial attitude. Each successive oscillation will be smaller than the one before it, until it eventually stabilizes.

An airplane with neutral dynamic stability will exhibit constant amplitude oscillations. The disturbances will neither increase nor decrease over time. For example, when a neutrally stable aircraft is initially pitched downwards, it will experience a temporary upward pitch before eventually returning to a downward pitch. These oscillations will continue indefinitely unless the pilot intervenes to stabilize the aircraft.

In the case of negative dynamic stability, an aircraft will encounter amplifying oscillations over time, indicating an unstable aircraft. After a disturbance, the deviations from the equilibrium state increase leading to progressively larger and more unpredictable movements away from the equilibrium state unless acted up on by the pilot.

Ensuring the safe and efficient completion of aircraft missions heavily relies on comprehending and handling aircraft stability. The performance of your aircraft ultimately depends on its design. The examples above indicate that an airplane that is dynamically stable must always be statically stable. Despite this, static stability alone is not enough to guarantee dynamic stability. Typically, static stability is the primary stability feature that is incorporated into an airplane's design[31].

For instance, as discussed above, training aircraft such as Cessna and Piper are constructed to be statically and dynamically stable, which allows for easy trimming and hands-off flying. However, fighter aircrafts such as F-22 are intentionally designed to be unstable, which allows them to be highly maneuverable and perform aggressive pitching, rolling and yawing easily. The stability and control of modern aircrafts are continuously improved by technological and design advancements.

## CHAPTER 2

### METHODOLOGY

#### 2.1 Geometry Configuration

In the early stages of our research, one of the primary challenges we faced was establishing a reliable geometric framework capable of accurately representing the complex flow phenomena associated with our study. To address this, we opted to create a three-dimensional (3D) model of the aircraft using SolidWorks, a powerful CAD software known for its precision and versatility in designing complex geometries [8].

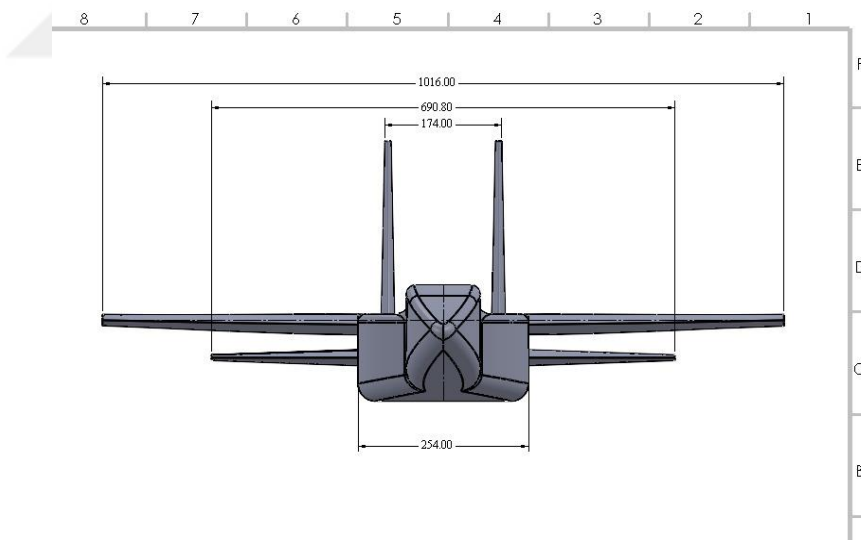


**Figure 2.1:** Wing and tail span dimensions in SolidWorks.

## 2.1.1 Vertical and Horizontal Tails Configuration

### Vertical Tail Geometry

Airfoil section

Tip.....	NACA 64-003.5
Root.....	NACA 64-005
Tip chord, cm.....	9.11
Root chord, cm .....	34.33
Taper ratio .....	375
Tail height (root to tip), cm.	25.40
$\Lambda_{le}$ , deg.....	36.52

### Horizontal Tail Geometry

Airfoil section

Tip.....	NACA64-002.5.
Root.....	NACA 64-005. 5
Tip chord, cm .....	5.08
Root chord, cm.....	24.50
Taper ratio .....	0.75
Span, cm	
Forward on body.....	69.09
Mid on body .....	69.08
Aft on body .....	67.81
$\Lambda_{le}$ , deg.....	50.0

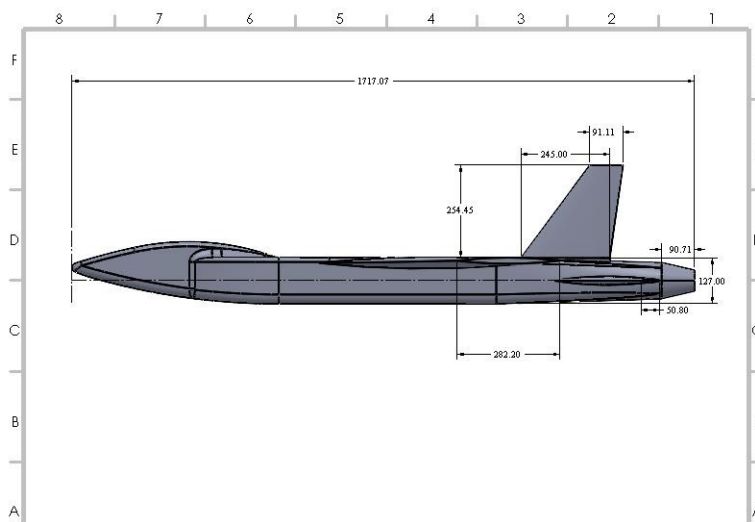


**Figure 2.2:** Dimensions of the VT, HT and the Nozzle.

### 2.1.2 Nose and Body Shape

The Twin engine model design features a circular cross-section at the nose, transitioning into a 1717mm long body with a rectangular fuselage that boasts rounded corners for enhanced aerodynamics and structural integrity.

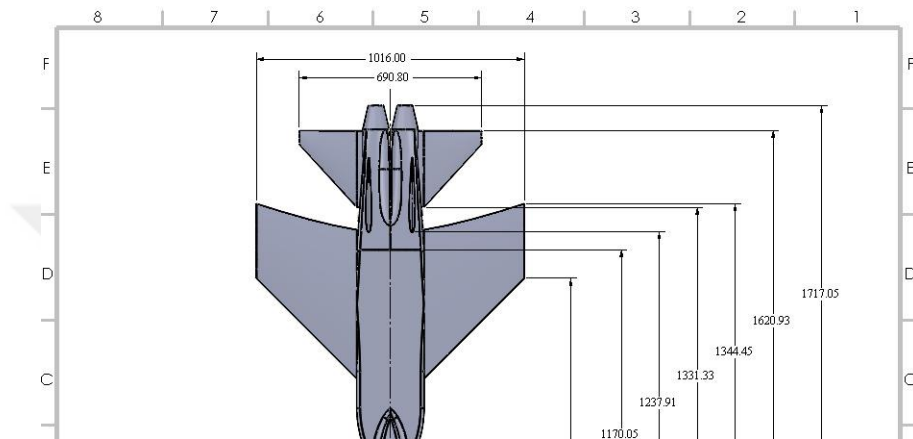


**Figure 2.3:** Lengths of the model from the nose.

### 2.1.3 Afterbody Configuration

The afterbody of the model, which is the primary focus of our study, extends from 1170.05 mm aft of the aircraft's nose to the nozzle exit plane. All simulations conducted concentrated on this specific section of the model.

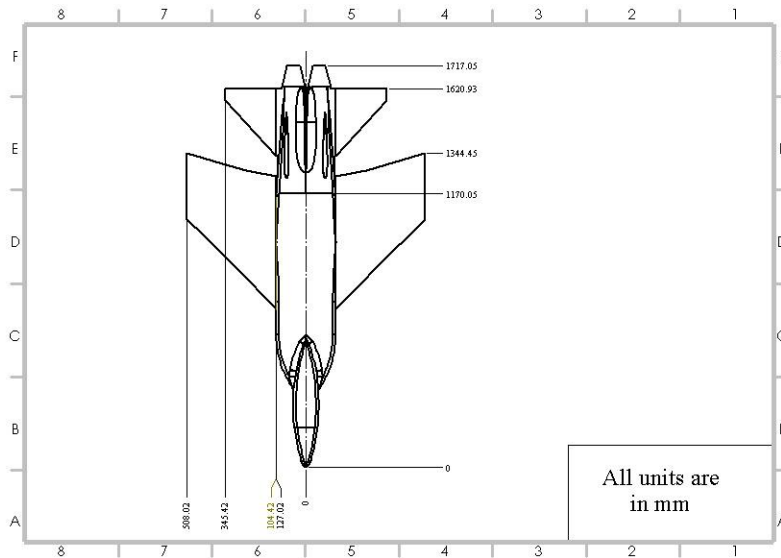


**Figure 2.4:** Afterbody dimensions in Solidworks.

## 2.2 Mesh Generation

In the analysis phase, the created CAD model is brought into the system and the enclosure is created. During the preprocessing stage, the geometric parameters (physical boundaries) of the problem are established. The fluid's volume is segmented into distinct cells, forming the mesh. Mesh generation is the process of dividing a geometric space into smaller, simpler elements, such as triangles or tetrahedral, for use in computational simulations[34].

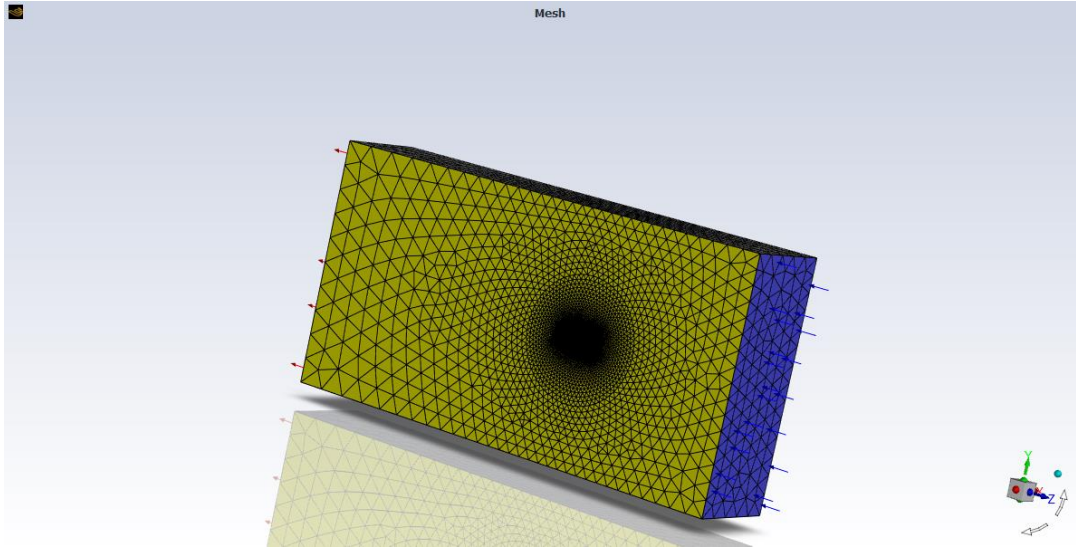


**Figure 2.5:** Mesh of the domain.

The creation of a fine mesh is essential for achieving valid and precise results. The mesh was generated utilizing the Gambit software. The domain mesh was successfully established prior to the creation of the aircraft mesh. The domain included inlet, interface, pressure far field, symmetry, twin engine and the outlet.

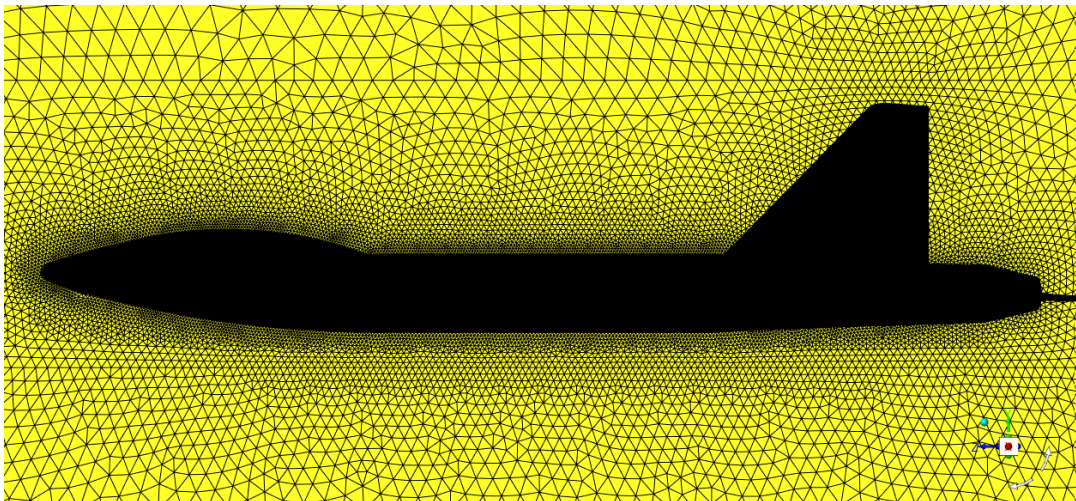


**Figure 2.6:** Side view of the surface mesh.

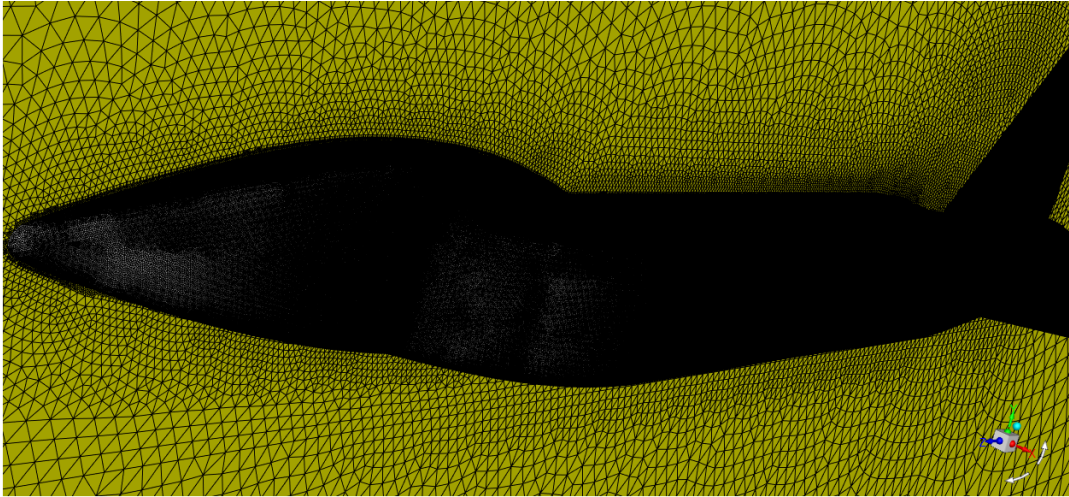


**Figure 2.7:** Front view of the surface mesh.

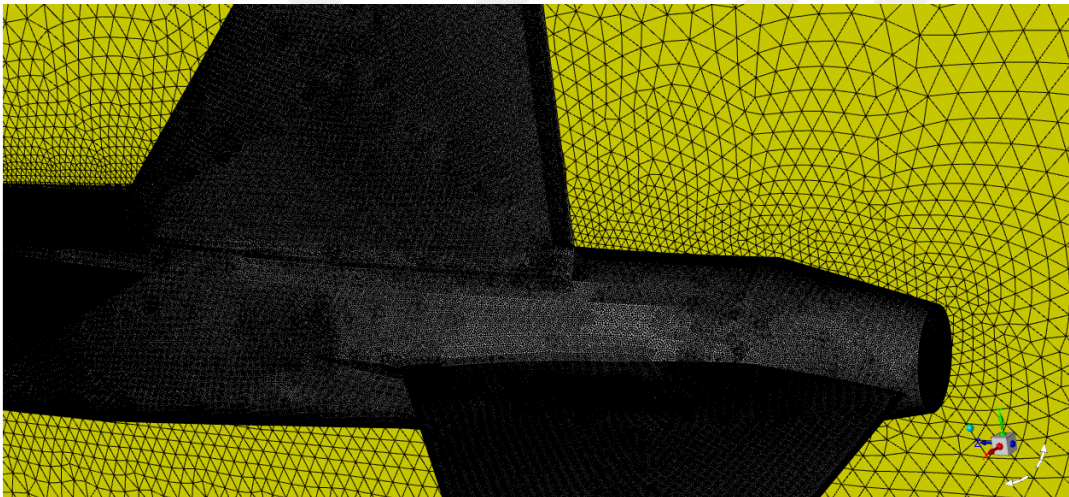


**Figure 2.8:** Rear view of the surface mesh.

### **2.3 Analysis Using Ansys Fluent**

Physical modeling encompasses the formulation of equations governing radiation, motion, enthalpy and species conservation. BC are established, which entails detailing the behavior and characteristics of the fluid at the problem's boundaries [35]. In the case of transient analyses, starting conditions are also specified. The simulation commences, and the equations are resolved through iterative methods, which may be conducted in either a steady-state or transient approach. In conclusion, a post-

processing tool is utilized for the examination and graphical representation of the resulting solution.

- **Turbulence Models:** The simulations employed the Spalart-Allmaras turbulence model. A density-based solver was utilized, given that all simulations involved compressible flow. Energy equations were incorporated to address the cases, as the nature of the simulations required consideration of compressibility.
- **Materials:** In this simulation, the working fluid was characterized as an ideal gas, as the boundary condition of "Pressure Far-field" was suitable for this classification. The analysis assumed that the twin-engine aircraft was operating under sea level conditions, with viscosity determined through the application of Sutherland's equations.
- **Boundary Conditions:** In this simulation, pressure far-field boundary conditions were implemented to represent a freestream compressible flow at an infinite distance, with the free-stream Mach numbers and static conditions clearly defined. The airplane was assigned with a "wall" boundary condition (Table 4.2).
- **Solution:** The employed solution technique was an Implicit method (refer to Table 4.3) utilizing the SIMPLE algorithm for pressure-linked equations. This method operates as an iterative process aimed at solving the equations related to velocity and pressure within a steady-state framework. The Courant number was established at 10, with under-relaxation factors set at 0.8 for both momentum and pressure, while the values for turbulent kinetic energy, turbulent dissipation rate, and turbulent viscosity were also fixed at 0.8. In terms of discretization, pressure was maintained as standard, whereas the parameters for Turbulent Dissipation Rate, Turbulent Kinetic Energy, Momentum, and Energy were configured to 2nd Order Upwind. Convergence monitoring throughout the solution process was conducted dynamically through the assessment of force coefficient values, rather than relying on the convergence of residuals. The findings were recorded, presented, and visually represented through graphs that illustrated the coefficients of lift, drag, and

moment, in addition to the residuals associated with the solution variables. In the Force Monitors, the force vectors for Lift and Drag were defined in relation to the free stream direction.

- **Iteration:** The iteration count was established at 10,000 within the designated Number of Iterations field. Subsequently, FLUENT initiated the calculations, commencing from iteration 1 and utilizing the initial solution. Following this, the graphs produced were created, printed, and stored in separate data files. The simulations were concluded once the graphs depicting the Coefficient of Lift versus iterations and the Coefficient of Drag versus iterations demonstrated convergence.

**Table 2.1: ANSYS Physics Setup-General.**

<b>GENERAL SETUP</b>	
Scale Domain extents	
X minimum = -15	X maximum = 60
Y minimum = 15	Y maximum = 15
Z minimum = -20	Z maximum = 20
<b>QUALITY REPORT</b>	
Orthogonal Quality Min	= 7.77685e – 03
Ortho Skew Min	= 9.67586e – 01
Aspect Ratio Min	4.22396e+01
<b>SOLVER</b>	
Type	Density Based
Formulation Velocity	Absolute
Time	Steady
<b>MODELS</b>	
Energy	On
Turbulence Model	Spalart-Allmaras
<b>MATERIALS</b>	
Fluid	Air
Density	1.225
Cp	1006.53
Thermal Conductivity	0.0241
Viscosity	1.7884e – 05
Solid	Aluminum
Density	2720
Cp	872
Thermal Conductivity	202.3

**Table 2.2: ANSYS Physics Setup- Cell Zone and Boundary Conditions**

<b>CONDITIONS OF CELL ZONE</b>	
Zone	Air
Type	Fluid
Operating Pressure	101325
<b>BOUNDARY CONDITIONS</b>	
Twin engine	Wall Stationary
Velocity Inlet – M	0.8 \$ 0.9
X – Component Direction of Flow	386.38
Y – Component Direction of Flow	103.528
Z – Component Direction of Flow	0
<b>REFERENCE VALUES</b>	
Area	1
Density	1.225
Enthalpy	0
Length	1000
Pressure	0
Temperature	0

**Table 2.3: ANSYS Physics Setup-Solutions.**

<b>SOLUTN</b>	
Formulatn	Implicit
Flux	Roe-FDS
<b>SPATIAL DISCRETIZATN</b>	
Gradient	least Squares Method
Flow	2nd Order Upwind
Turbulent Kinetic Energy	2nd Order Upwind
Turbulent Dissipation Rate	2nd Order Upwind
<b>CONTROLS OF SOLUTION</b>	
Courant Nnbr	10
<b>FACTORS UNDER RELAXATION</b>	
Turbulent Kinetic Energy	0.8
Turbulent Dissipation Rate	0.8
Turbulent Viscosity	0.8
Solid	1
<b>LIMITS OF SOLUTION</b>	
Min Absolute Pressure	1
Max Absolute Pressure	5e+10
Min Static Temperature	1
Max Static Temperature	5000
Min Turbulent Kinetic Energy	1e-14
Min Turbulent Dissipation Rate	1e-20
Max Turbulent Viscosity Ratio	
Positivity Rate Limit	0.2
<b>MONITORS</b>	
Residuals – Criteria of Convergence	$10^{-6}$
Dynamic Pressure, Energy, Turbulent Dissipation Rate, Static Pressure, Turbulent Kinetic	Twin Engine
<b>INITIALIZATION OF SOLUTION</b>	
Nmbr of Iterations	10000
Interval of reporting	1
Case Check	Ok – Calculation Run.

## CHAPTER 3

### RESULTS AND DISCUSSION

#### 3.1 Modeling of Conceptual Configuration

The model used for this analysis is a generic, twin-engine, twin-tail, high-wing fighter with a  $45^\circ$  swept wing, which was designed and fabricated at the NASA- Langley Research Center. This fighter was used for many years as a reference model and it was tested extensively in other studies and wind tunnels[10], [11]. The Solidworks model was generated based on the configuration of this fighter in the AGARD Advisory Report N° 303Vol I at the Langley Transonic wind tunnel data testing [8]. The geometry of the test case features a vertical tail in forward position horizontal tail in mid position as it is shown in figure 1.1 and a schematic of the test case is shown in figure 5.1.

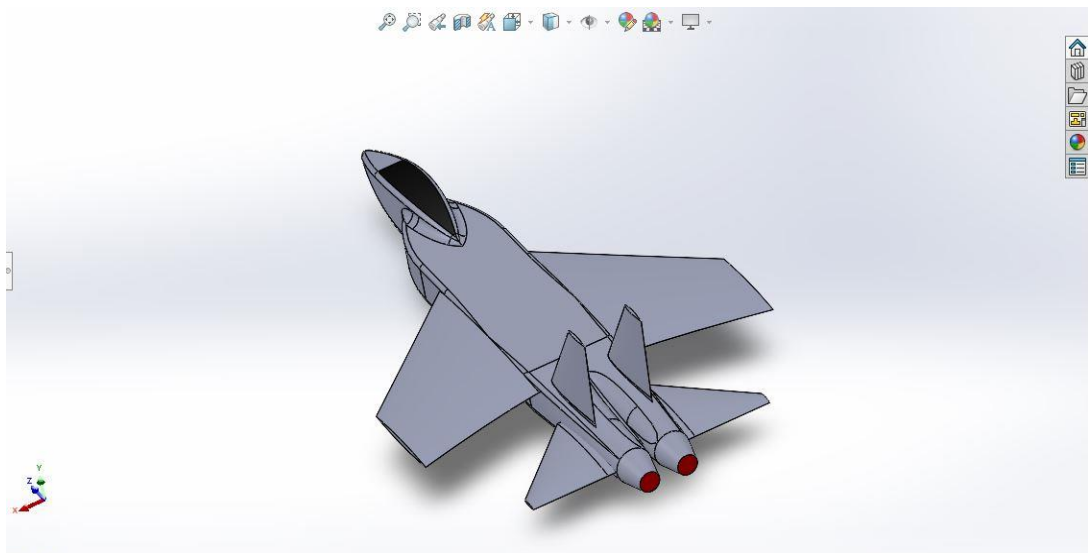


**Figure 3.1:** A 3D Sketch view of the twin Engine afterbody Model in SolidWorks.

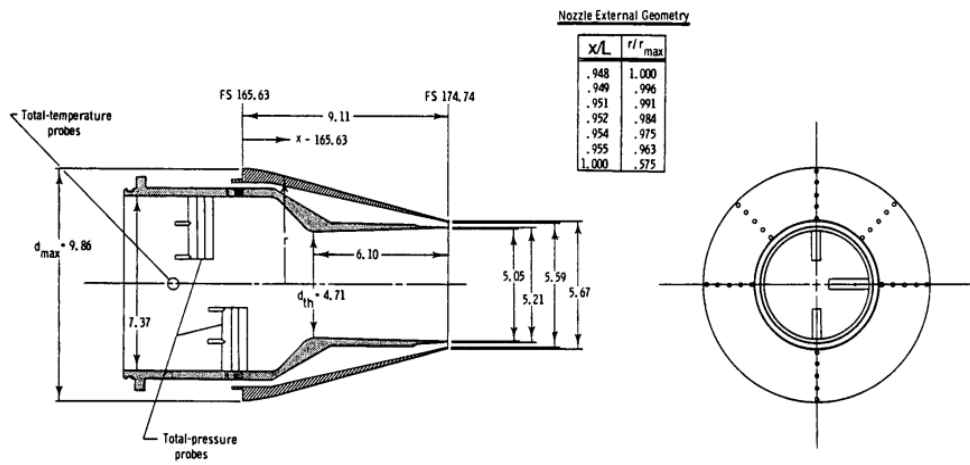


**Figure 3.2.** Convergent-Divergent Nozzle Geometric Details in cm.

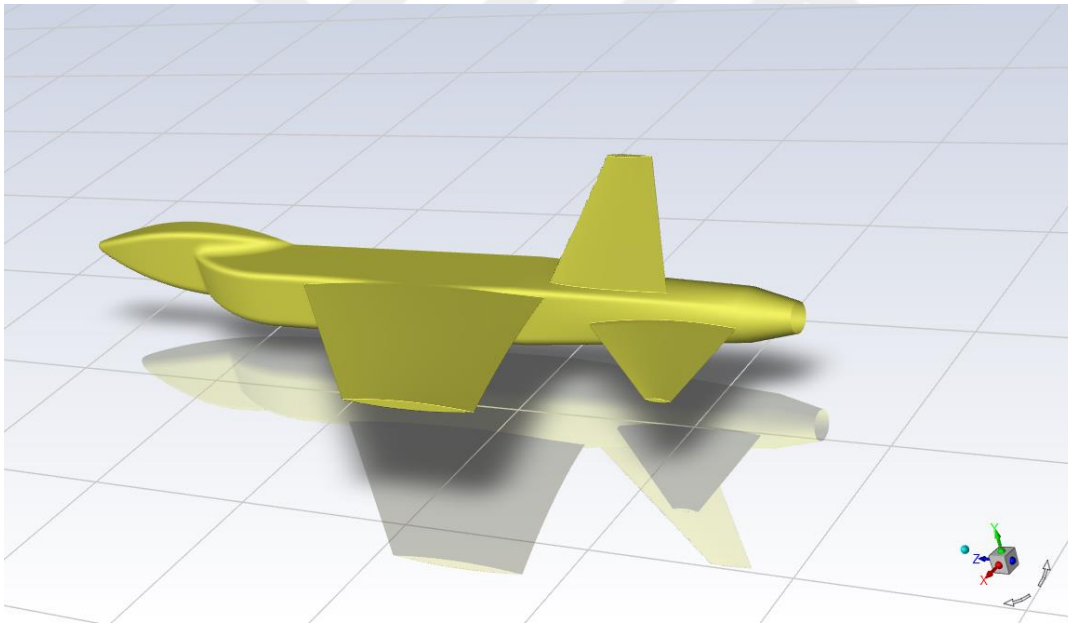


**Figure 3.3:** Half body view of a Twin Engine Afterbody model in Fluent featuring a forward vertical and mid horizontal tails.

### 3.2 Simulation (Computational) Details

The computations in this study were obtained using density based solver type and Spalart-Allmaras as turbulence model. The boundary conditions are defined by applying a pressure far from the field to the external surfaces of the domain, while a symmetry condition is enforced on the plane of symmetry located within the domain. The variables of density, pressure, momentum, turbulent kinetic energy, energy, and specific dissipation rate are all set to utilize second-order upwind schemes. Viscosity is calculated in accordance with Sutherland's law, whereas density is presumed to adhere to the ideal gas law. Moreover, the coefficients of aerodynamic are tracked in accordance with a convergence criterion of  $10^{-6}$ . The freestream conditions for total temperature and pressure were 300K and 101325 Pa respectively. The aircraft is subjected to the wall condition, while the duct intake surface is given condition of inlet velocity. The remaining analysis is conducted with a no-slip condition.

The simulations were done on Mach number 0.8 and 0.9 at nozzle pressure ratio of 3.4 nearing the 3.54 of the fully expanded NPR and at different circumferential positions of pressure orifice rows ( $\theta = 180^\circ, 225^\circ$  and  $240^\circ$ ) and AoA of  $0^\circ$ . The Reynolds number for the computations at Mach number 0.8 was about 19 million while for Mach number 0.9 was about 23 million. The final dimensions of grid for a specific model consists of 7 to 9 million elements while the number of cells for the mesh is 12 million. All these computations were carried out on LG Intel Xeon 2.2 GHz workstation.

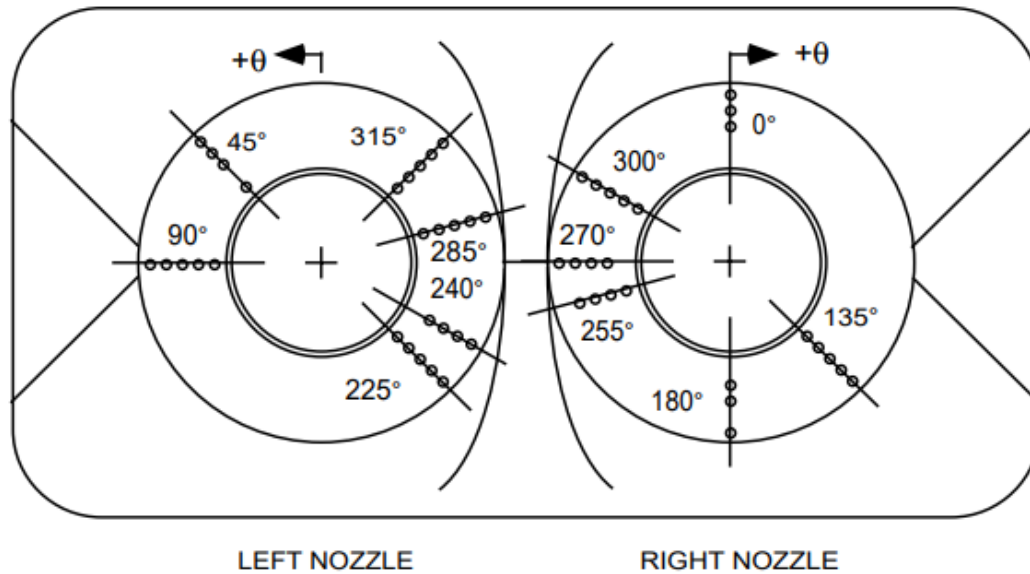


**Figure 3.4:** Circumferential Positions of Pressure Orifice rows for Left and Right Nozzles.

### 3.3 Results of the Study

In this study, the medium location of the HT and the forward location of the VT of the twin engine afterbody model fighter aircraft serve as the basis for the experimental data collection as well as our computational data. We compared our results with the experimental data for the  $C_p$  on the A/B surface at different circumferential locations of the pressure orifice rows ( $\theta = 180^\circ, 225^\circ$  and  $240^\circ$ ) for Mach number 0.8 and 0.9 as described in section 5.2 with respect to normalized axial location ( $x/L$ ).

#### 3.3.1 Pressure Coefficient ( $C_p$ ) plots

The static pressure coefficient, denoted as  $C_p$ , is illustrated on the afterbody at several circumferential positions ( $\theta = 180, 225$  and  $240$  degrees) for Mach numbers of 0.8 and 0.9 and Nozzle Pressure Ratio of 3.4. The experimental measurements were obtained from the midpoint of the horizontal tail and the forward position of the vertical tail. For the purpose of obtaining accurate results for both the experimental and

computation data, it was assumed that the afterbody starts from  $x = 1717$  mm or  $x/L=0.7$  and later, the evaluations of pressure were done from  $x/L = 0.7$  and on.

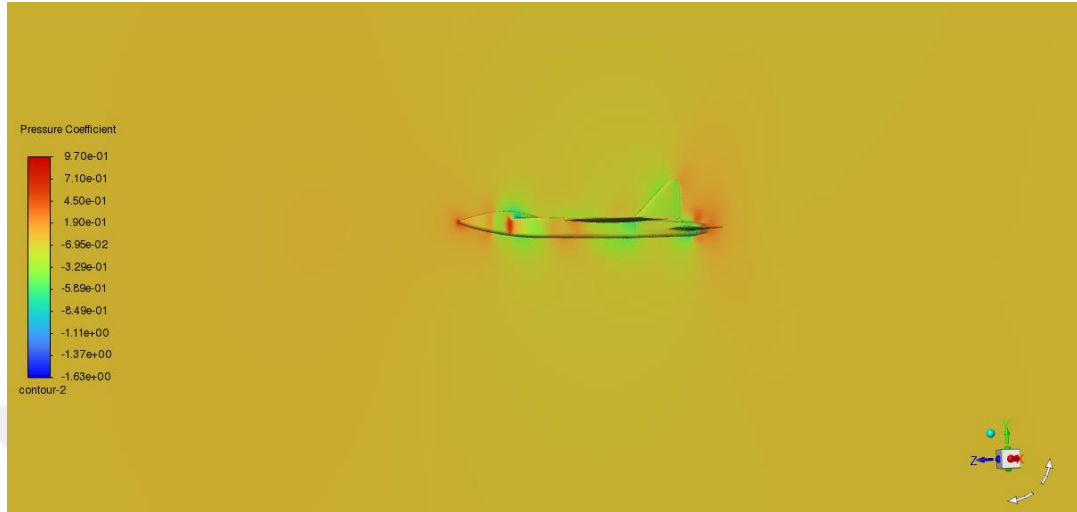


**Figure 3.5:** Contour of Pressure Coefficient at  $M=0.8$ .

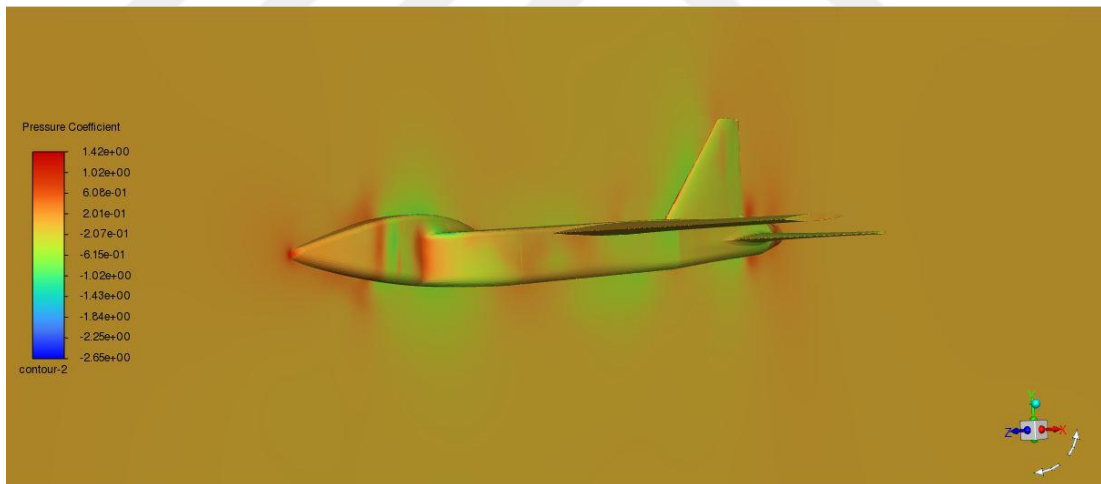


**Figure 3.6:** Contour of Pressure Coefficient at  $M=0.9$ .

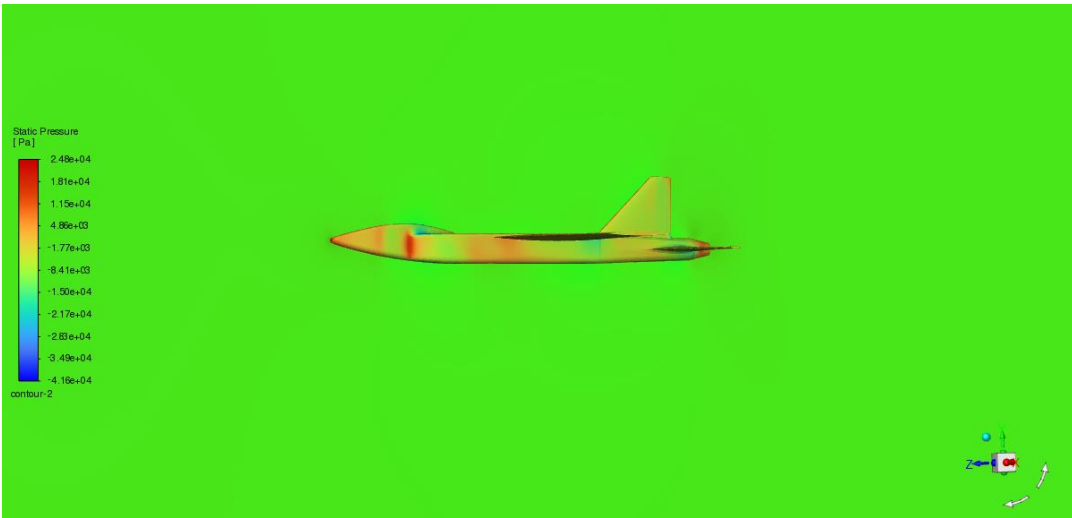


**Figure 3.7:** Contour of Static Pressure at  $M = 0.8$ .



**Figure 3.8:** Contour of Static Pressure at  $M = 0.9$ .

Figure 3.9 – 3.14 presents a comparative analysis of computational and experimental data concerning the pressure coefficients on the surface of an axisymmetric twin-engine fighter. The horizontal axis illustrates the axial distance measured downstream from the nose ( $x$ ), normalized by the model length ( $L$ ), whereas the vertical axis depicts the pressure coefficients ( $c_p$ ).

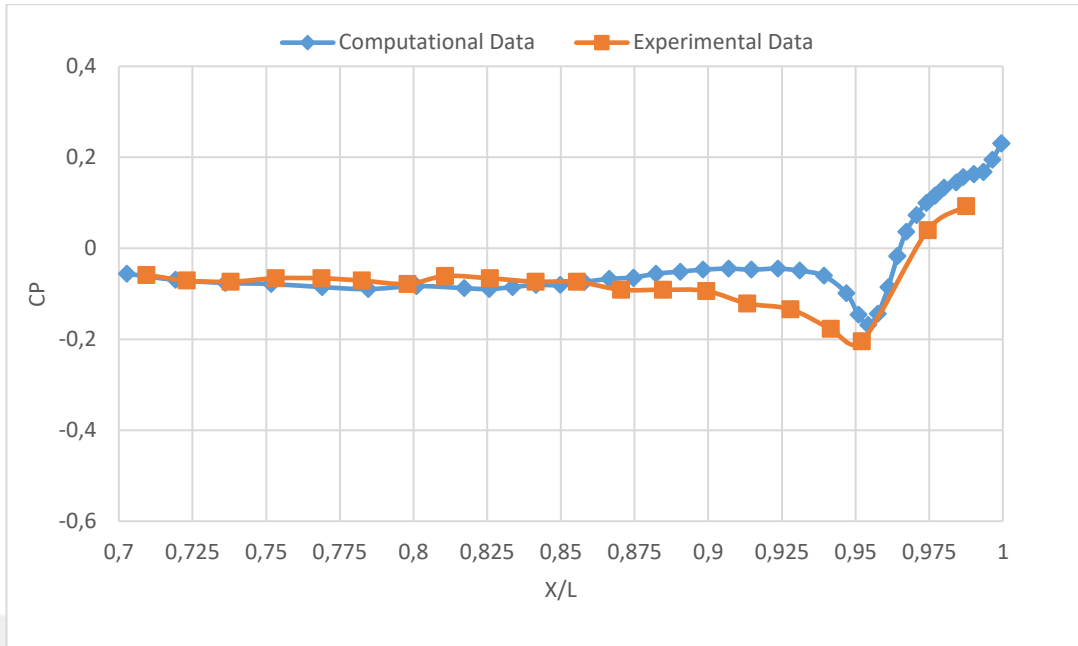


**Figure 3.9:** Cp plots for  $M = 0.8$ ,  $NPR = 3.4$  and  $\theta = 180^\circ$

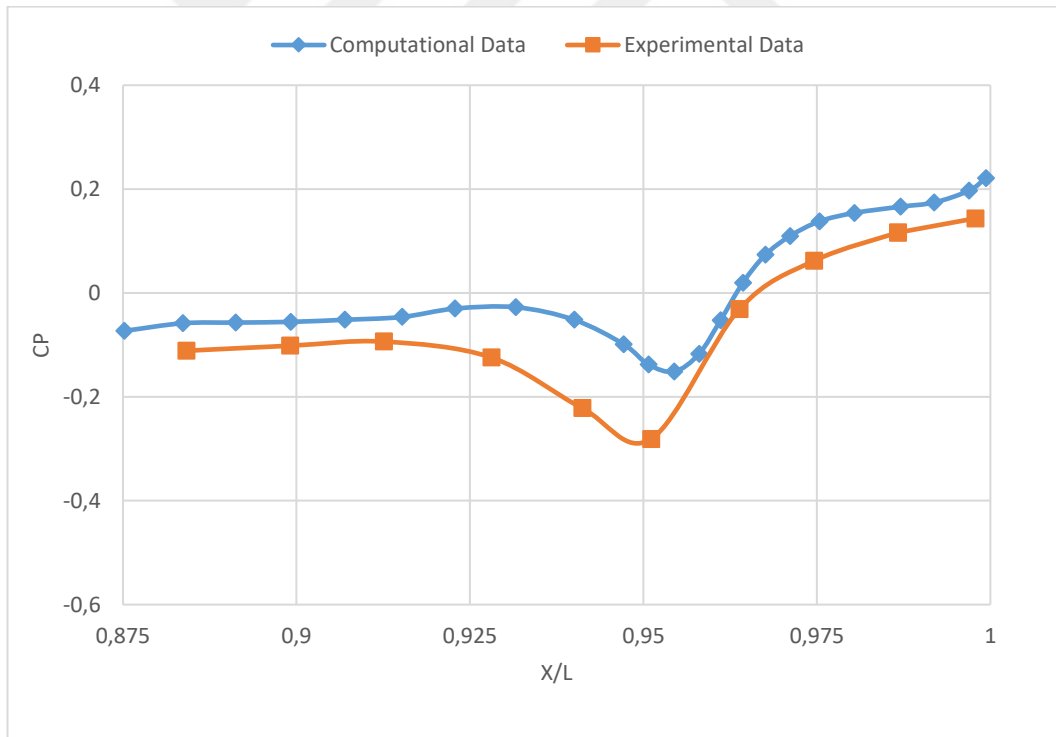


**Figure 3.10:** Cp plots for  $M = 0.8$ ,  $NPR = 3.4$  and  $\theta = 225^\circ$

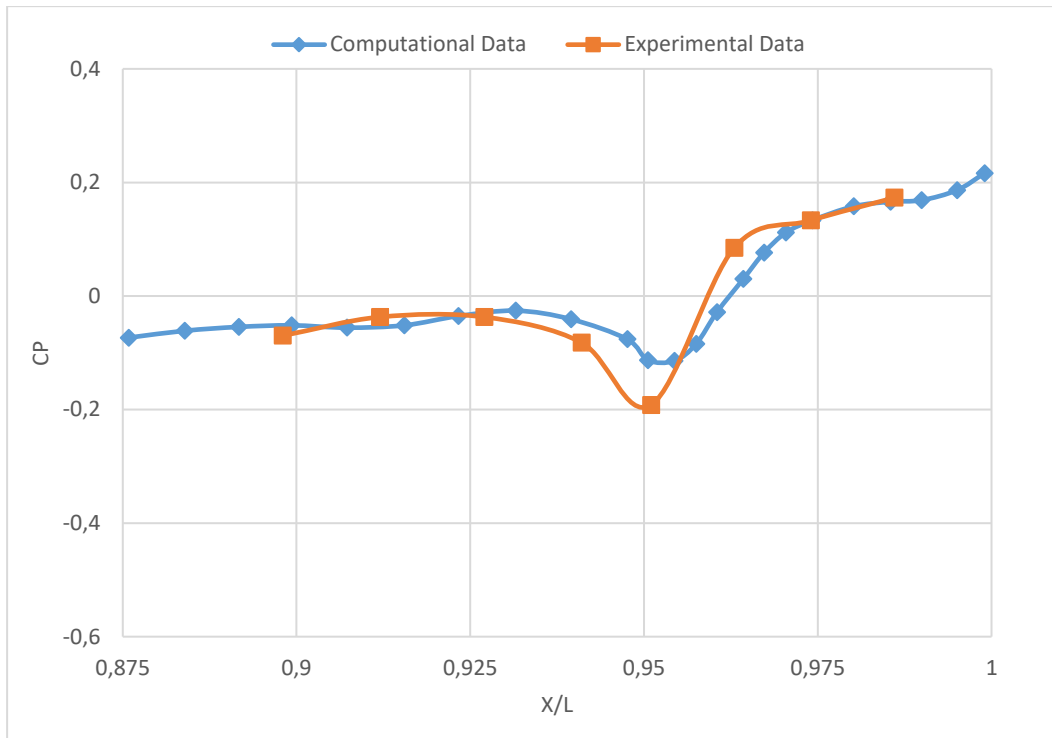


**Figure 3.11:** Cp plots for  $M = 0.8$ ,  $NPR = 3.4$  and  $\theta = 240^\circ$

The graphs (Figure 3.9 – 3.11) illustrate the comparison of the pressure coefficient ( $C_p$ ) vs. Normalized Axial Location ( $x/L$ ) between computational data and experimental data at different circumferential positions ( $\theta$ ) of the afterbody of the fighter aircraft at a Mach number of 0.8 and a nozzle pressure ratio of 3.4.

In figure 5.9, with  $\theta = 180^\circ$ , the  $C_p$  distribution shows that both the computational and experimental data remain relatively constant along most of the  $x/L$  axis. However, a notable divergence occurs as  $x/L$  approaches 1, where the computational data predicts a significant increase in  $C_p$  compared to the experimental data. This divergence suggests that at this circumferential position, the computational model may be overestimating the pressure rise near aft end of the model.

In the graphs (figure 3.10 and figure 3.11), representing  $\theta = 240^\circ$  and  $\theta = 225^\circ$  respectively, the  $C_p$  profiles exhibit a similar trend with consistent data up to around  $x/L = 0.95$ . Beyond this point, both sets of data show a significant decrease in  $C_p$ , followed by a rise as  $x/L$  approaches 1. However, the computational data consistently

shows a higher  $C_p$  compared to the experimental data, particularly near the aft end of the model. This indicates that while the computational model captures the general trend of the pressure distribution, it tends to overpredict the pressure in the aft region of the model.

Overall, the comparison highlights a systematic discrepancy between the computational and experimental results, especially near the aft end of the model at higher circumferential angles. This could point to potential areas for improving the computational model, possibly by refining the turbulence modeling or boundary conditions to better capture the complex flow phenomena occurring in this region.

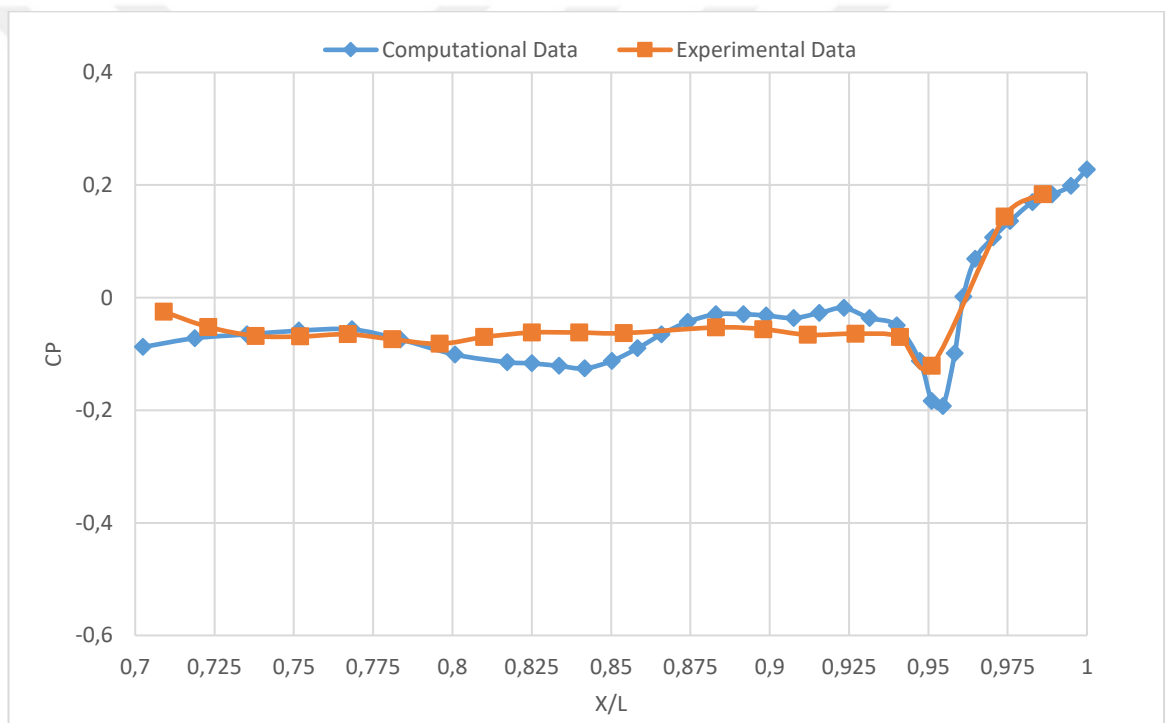


**Figure 3.12:**  $C_p$  plots for  $M = 0.9$ ,  $NPR = 3.4$  and  $\theta = 180^\circ$

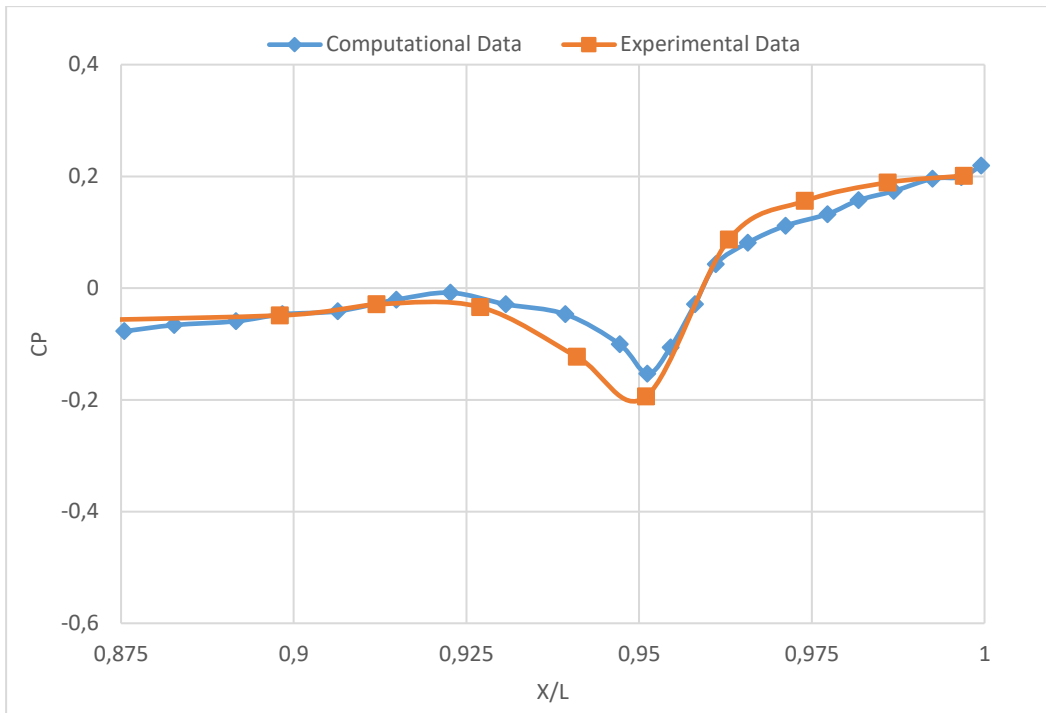


**Figure 3.13:** Cp plots for M = 0.9, NPR = 3.4 and  $\theta = 225^\circ$

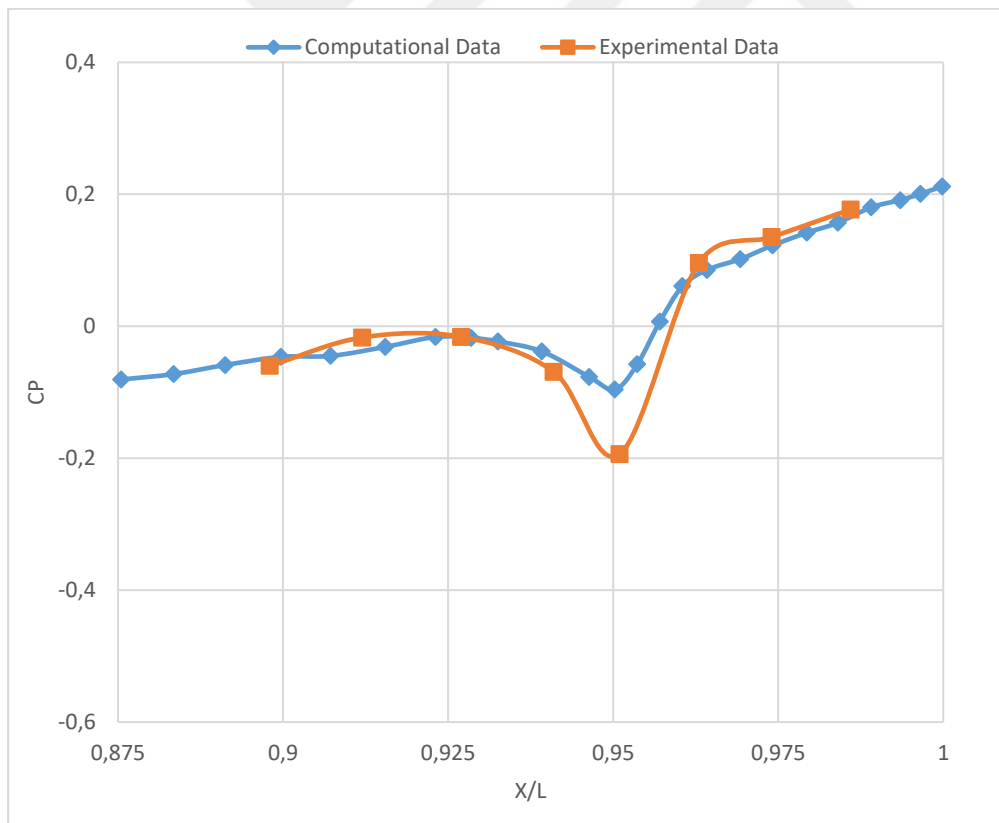


**Figure 3.14:** Cp plots for M = 0.9, NPR = 3.4 and  $\theta = 240^\circ$

The graphs (Figure 3.12 - 3.14) depict the Pressure Coefficient ( $C_p$ ) vs. Normalized Axial Location ( $x/L$ ) for a Mach number ( $M$ ) of 0.9 and a Nozzle Pressure Ratio (NPR) of 3.4 at different circumferential positions of pressure orifice rows ( $\theta$ ). The positions shown are  $\theta=180^\circ$ ,  $\theta=225^\circ$ , and  $\theta=240^\circ$ . Across all three graphs, both computational data and experimental data follow similar trends, with discrepancies becoming more pronounced towards the aft end of the model (around  $x/L=0.95$ ).

For  $\theta=180^\circ$ , the  $C_p$  values are relatively stable until  $x/L \approx 0.95$ , where both computational and experimental data show a sharp dip followed by an increase, though computational values show a more pronounced change. At  $\theta=225^\circ$  and  $\theta=240^\circ$ , the patterns are similar, but the match between computational and experimental data is closer. At these circumferential positions, the computational data dips slightly deeper around  $x/L=0.95$  and rises more sharply after, while the experimental data shows a more gradual change. This indicates that while the computational model is generally reliable, its accuracy decreases in capturing the precise pressure distribution changes, especially in the regions affected by complex aerodynamic phenomena such as separation and wake.

### 3.3.2 Mach Number Plots

Figures 3.15 and 3.16 illustrate the Mach number distribution along the symmetry plane for Mach 0.8 and 0.9 at a nozzle pressure ratio (NPR) of 3.4 with an angle of attack ( $\alpha$ ) set to zero. The plot reveals how the Mach number varies across the plane, reflecting the changes in flow dynamics under the specified conditions. At Mach 0.8, the flow is likely subsonic throughout most of the domain, with potential regions of acceleration near the nozzle exit. In contrast, the plot for Mach 0.9 demonstrates a near-sonic flow that may approach or reach supersonic speeds, particularly in areas of expansion or near the nozzle exit. This comparison highlights the impact of increasing the Mach number on the flow characteristics, showcasing the effects on the velocity distribution and potential shock formations within the flow field.

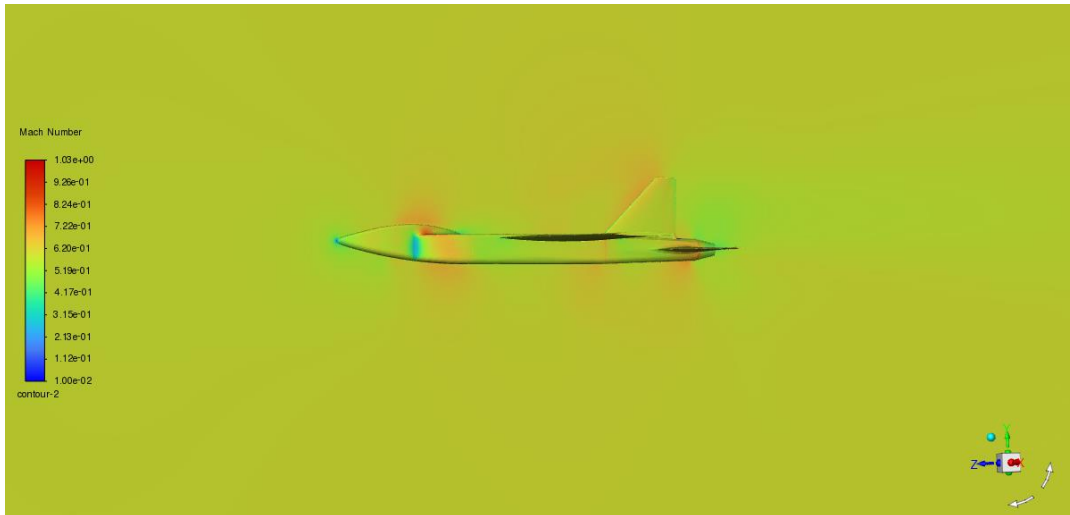


**Figure 3.15:** Mach Number Contour at  $M = 0.8$  and  $NPR = 3.4$ .

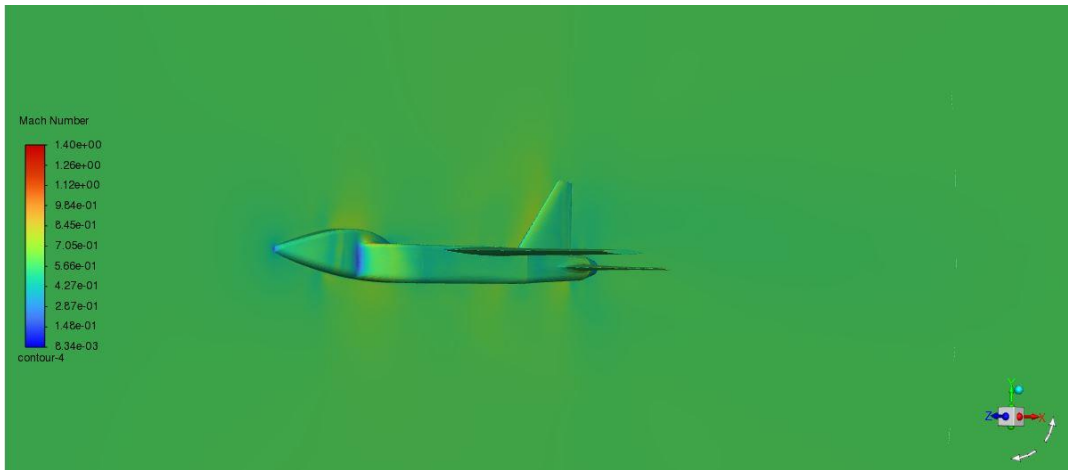


**Figure 3.16:** Mach Number Contour at  $M = 0.9$  and  $NPR = 3.4$

## CHAPTER 4

### CONCLUSION

#### 4.1 Overall Conclusion

The research conducted in this thesis represents a significant effort to compare CFD simulations with data acquired through experimentation from the Langley Transonic Wind Tunnel. By focusing on the pressure distribution around the nozzle of a twin-engine aircraft afterbody model, the study aims to assess the precision of simulations done with CFD under specific flight conditions. This comparison is crucial for understanding the reliability of CFD tools in predicting aerodynamic performance, particularly in complex flow regions where intricate phenomena such as shock waves and boundary layer separation occur.

In order to investigate the aerodynamic behavior of the twin engine aircraft's nozzle and afterbody, a simple 3-DoF twin engine model has been constructed. The findings demonstrate that while CFD simulations generally align with experimental data, notable discrepancies emerge, particularly near the aft end of the model at higher circumferential angles. The computational model tends to overestimate  $C_p$  in these regions, suggesting potential limitations in the current CFD methods. These discrepancies highlight the need for further refinement in turbulence modeling and boundary condition settings to enhance the fidelity of CFD simulations. The systematic overprediction observed in the simulations indicates that the computational model may not fully capture the intricate flow dynamics present in the experimental setup.

Specifically, the analysis at  $\theta=180^\circ$ ,  $\theta=225^\circ$ , and  $\theta=240^\circ$  reveals that the computational data tends to deviate significantly from the experimental results as  $x/L$  approaches 1. This trend is consistent across different  $M$  (0.8 and 0.9) and NPR (3.4), emphasizing the robustness of the observed discrepancies. The divergence is more pronounced at higher circumferential angles, where complex flow phenomena are likely to be more influential. This finding underscores the importance of accurately modeling the aft region of the A/B, which is critical for the overall aerodynamic performance of the aircraft.

The systematic differences observed between the CFD simulations and the wind tunnel data suggest areas for potential improvement in the computational models. Enhancements in turbulence modeling, particularly in capturing separation and wake effects, are essential for reducing the observed discrepancies. Additionally, refining the boundary conditions to better replicate the experimental setup could improve the accuracy of the simulations. Addressing these areas will not only enhance the predictive capability of CFD tools but also contribute to more reliable and efficient aerodynamic designs for advanced aircraft configurations.

In conclusion, this thesis provides valuable insights into the accuracy and limitations of CFD simulations in predicting aerodynamic performance. The numerical results in this study are in good consistent with the experimental study results from the Langley Transonic Wind Tunnel. By identifying specific areas for improvement, this study paves the way for future research aimed at enhancing the precision of aerodynamic forecasts. Such advancements are crucial for the development of more efficient and reliable twin-engine aircraft designs, ultimately contributing to the advancement of aerospace engineering and technology.

## **4.2 Future work**

Future research should focus on expanding the range of  $M$  and NPR to thoroughly understand the  $C_p$  distribution along  $x/L$  for various flight conditions. This includes testing at higher and lower Mach numbers, as well as different nozzle configurations and geometries, to capture a broader spectrum of aerodynamic behaviors. Additionally, integrating advanced CFD simulations with high-fidelity turbulence

models and experimental validations at various  $\theta$  will enhance the predictive accuracy of  $C_p$  distributions. These efforts will contribute to the optimization of A/B designs for improved aerodynamic performance and fuel efficiency in modern fighter aircraft.

Furthermore, the impact of environmental factors such as temperature, altitude, and atmospheric conditions on the pressure coefficient should be investigated. Understanding how these variables influence  $C_p$  can lead to more robust and adaptable aircraft designs capable of maintaining performance across diverse operational environments. Additionally, exploring the interaction between the aircraft's A/B and other aerodynamic surfaces, such as wings and control surfaces, can provide insights into minimizing drag and improving overall aircraft stability. Collaborative efforts between computational and experimental aerodynamics, leveraging cutting-edge technologies like machine learning for data analysis, will be pivotal in advancing the aerodynamic efficiency and performance of next-generation fighter aircraft.

## REFERENCES

- [1] W. Siddiqui, H. Naseer, S. M. Zahid, A. Maqsood, S. Salamat, and R. Riaz, 'Computational aerodynamics study of competing conceptual designs for advanced tactical fighter aircraft', *Journal of Aerospace Technology and Management*, vol. 13, 2021, doi: 10.1590/JATM.V13.1214.
- [2] D. P. Raymer, *Aircraft design : a conceptual approach*. 2018.
- [3] Egbert Torenbeek, 'ADVANCED AIRCRAFT DESIGN: Conceptual Design, Analysis and Optimization of Subsonic Civil Airplanes', 2012.
- [4] A. Elsayed *et al.*, 'Conceptual design of a supersonic multifunctional military aircraft'.
- [5] A. Kumar Kundu, 'Aircraft design', 2010. [Online]. Available: [www.cambridge.org/Kundu](http://www.cambridge.org/Kundu)
- [6] R. C. Nelson, *Flight stability and automatic control*. WCB/McGraw Hill, 1998.
- [7] S. Ozdemir, M. Tuna, S. C. İnel, and S. Özdemir, 'Longitudinal Stability Analysis of Aircrafts', *Journal of Scientific and Engineering Research*, vol. 179, no. 10, pp. 45–51, 2020, [Online]. Available: [www.jsaer.com](http://www.jsaer.com)
- [8] David J. Wing, 'Twin Engine Afterbody Model', 1994.
- [9] U. Ahmed, '3-DOF Longitudinal Flight Simulation Modeling And Design Using MATLAB/SIMULINK', 2012.
- [10] D. J. Wing, 'Afterbody/Nozzle Pressure Distributions of a Twin-Tail Twin-Engine Fighter With Axisymmetric Nozzles at Mach Numbers From 0.6 to 1.2', 1995. [Online]. Available: <http://techreports.larc.nasa.gov/ltrs/ltrs.html>
- [11] L. D. Leavitt, 'Effect of Empennage Location on Twin-Engine Afterbody/Nozzle Aerodynamic Characteristics at Mach Numbers From 0.6 to 1.2', 1958. [Online]. Available: <https://ntrs.nasa.gov/search.jsp?R=19830017395>

- [12] A. M. Kamal and A. Ramirez-Serrano, ‘Systematic methodology for aircraft concept development with application to transitional aircraft’, in *Journal of Aircraft*, American Institute of Aeronautics and Astronautics Inc., 2020, pp. 179–197. doi: 10.2514/1.C035437.
- [13] M. Figat and A. Kwiek, ‘Analysis of longitudinal dynamic stability of tandem wing aircraft’, *Aircraft Engineering and Aerospace Technology*, vol. 95, no. 9, pp. 1411–1422, Sep. 2023, doi: 10.1108/AEAT-11-2022-0328.
- [14] L. Malik and A. Tevatia, ‘Comparative analysis of aerodynamic characteristics of F16 and F22 combat aircraft using computational fluid dynamics’, *Def Sci J*, vol. 71, no. 2, pp. 137–145, Mar. 2021, doi: 10.14429/DSJ.71.15762.
- [15] R. A. Johansen and N. Mourtos, ‘Conceptual Design for a Supersonic Advanced Military Trainer’, 2019.
- [16] D. Kiran and A. R. Çete, ‘DEVELOPMENT AND VERIFICATION OF A MULTIBLOCK STRUCTURED GRID SOLVER FOR 3D EULER/NAVIER-STOKES EQUATIONS’. [Online]. Available: <https://dergipark.org.tr/tr/pub/muhendismakina>
- [17] W. F. Phillips, ‘Mechanics of Flight’, 2004.
- [18] ‘Aircraft Performance Database > F14’. Accessed: Jul. 08, 2024. [Online]. Available: <https://contentzone.eurocontrol.int/aircraftperformance/details.aspx?ICAO=F14&GroupFilter=5>
- [19] ‘Aircraft Performance Database > F15’. Accessed: Jul. 08, 2024. [Online]. Available: <https://contentzone.eurocontrol.int/aircraftperformance/details.aspx?ICAO=F15&GroupFilter=5>
- [20] ‘Panavia Tornado ADV (Air Defense Variant) Air Defense Fighter / Interceptor Aircraft’. Accessed: Jul. 08, 2024. [Online]. Available: [https://www.militaryfactory.com/aircraft/detail.php?aircraft\\_id=54](https://www.militaryfactory.com/aircraft/detail.php?aircraft_id=54)

- [21] ‘Suchoi / Sukhoi Su-15 - Specifications - Technical Data / Description’. Accessed: Jul. 08, 2024. [Online]. Available: [https://www.flugzeuginfo.net/acdata\\_php/acdata\\_su15\\_en.php](https://www.flugzeuginfo.net/acdata_php/acdata_su15_en.php)
- [22] ‘Aircraft Performance Database > MG29’. Accessed: Jul. 08, 2024. [Online]. Available: <https://contentzone.eurocontrol.int/aircraftperformance/details.aspx?ICAO=MG29&GroupFilter=5>
- [23] ‘Aircraft Performance Database > MG31’. Accessed: Jul. 08, 2024. [Online]. Available: <https://contentzone.eurocontrol.int/aircraftperformance/details.aspx?ICAO=MG31&GroupFilter=5>
- [24] ‘Lockheed Martin F-22 Raptor 5th Generation Air Dominance Fighter’. Accessed: Jul. 03, 2024. [Online]. Available: [https://www.militaryfactory.com/aircraft/detail.php?aircraft\\_id=20](https://www.militaryfactory.com/aircraft/detail.php?aircraft_id=20)
- [25] ‘Aircraft Performance Database > F18’. Accessed: Jul. 08, 2024. [Online]. Available: <https://contentzone.eurocontrol.int/aircraftperformance/details.aspx?ICAO=F18&GroupFilter=5>
- [26] M. A. C. Hasenau, S. A. Varga, A. E. Scholz, and M. Hornung, ‘ENHANCEMENT OF AN AIRCRAFT DESIGN ENVIRONMENT FOR THE DESIGN OF FIGHTER AIRCRAFT’, 2021, doi: 10.25967/550024.
- [27] Z. Amador, ‘Conceptual Design And Analysis Of A Supersonic fighter With Lowboom Technology’, 2022.
- [28] MIL-STD-3013, ‘GLOSSARY OF DEFINITIONS, GROUND RULES, AND MISSION PROFILES TO DEFINE AIR VEHICLE PERFORMANCE CAPABILITY’, 2003. [Online]. Available: <http://www.everyspec.com><http://www.everyspec.com>
- [29] J. A. Schwartz, ‘FIGHTER AIRCRAFT DESIGN SYSTEM USER’S MANUAL’, 1988.

- [30] H. Peiris, P. Nirmal, H. Bandara, D. Mahindarathne, S. Rangajeeva, and R. Bandara, 'Aerodynamics Analysis of F-16 Aircraft', 2015.
- [31] D. geete, 'CFD Analysis of conceptual Aircraft body', 2017. [Online]. Available: [www.irjet.net](http://www.irjet.net)

